General

We would like to thank the anonymous Referees for providing valuable comments to improve and clarify our manuscript. We revised our manuscript to fully accommodate the Referees' comments. Please find our responses (shown in bold) to the specific comments of Referee #1 and #2, and the descriptions of changes (in bold italic) made in the revised manuscript below. Page and line numbers of the described changes refer to the revised manuscript without markings. The marked-up version of the revised manuscript is attached to the end of this file. All changes in the revised manuscript are marked using the function "Track Changes" of Microsoft Word.

Comments of Referee #1 and our responses to them

Comment

This paper describes a method of splicing together in situ measurements from ships, from aircraft, and from the ACTM model to create vertical profiles of CO2 over the Pacific Ocean. The vertical profiles are integrated to calculate XCO2 values that are then compared with the OCO-2, ACOS-GOSAT, and NIES-GOSAT retrievals over the same region. It's not clear to me whether ACP is the correct journal for this publication; it seems as though AMT might be a better fit for the paper's stated goals.

Response

Our manuscript, which describes a method to derive XCO_2 by using ship, aircraft and model data, doesn't intend to solely focus on the technical and theoretical aspects (with a rigorous uncertainty analysis). In addition to the technical aspects, our manuscript presents a detailed analysis of the spatiotemporal variations of CO_2 of each in situ and satellite dataset over the Pacific Ocean (section 4.1 and 4.2). Furthermore, using the new constructed observation-based XCO_2 dataset, we demonstrate its application as a reference for XCO_2, which is not only of relevance for validating satellite data, but especially for carbon cycle studies. As a complement to TCCON data, we believe that the applicability as reference for XCO_2 over oceans is of immediate relevance to a wide interdisciplinary scientific audience in atmospheric chemistry and physical sciences. Because our goal is beyond the primarily technical aspects, we believe that ACP is a more appropriate journal than AMT.

General comments

Comment

There are multiple ATom and HIPPO profiles throughout the Pacific – it would very much strengthen this paper if you could find coincident data with HIPPO/ATom profiles and compare vertical profiles in detail.

Response

We fully agree with the Referee #1 that HIPPO (Hiaper Pole-to-Pole Observations) and ATom (Atmospheric Tomography Mission) profiles would be very valuable to strengthen our results. However, coincident profile data of the HIPPO and ATom campaigns between the years 2014 and 2017 and in the longitude–latitude range of 130° E to 173° E and 30° S to 40° N do not exist. The newest dataset of HIPPO covers the year 2011 (HIPPO 4, HIPPO 5, https://www.eol.ucar.edu/node/3402, 12/21/2020). Data from the Atom 1 campaign cover the time period from 07/29/2016 to 08/23/2016 (https://daac.ornl.gov/cgi-bin/dsviewer.pl?ds_id=1581, 12/21/2020). Unfortunately, the flight tracks closest to our study region are generally more than 20° east of it (Figure R1, purple line). The lack of coincident data is a drawback in strengthening our results, but emphasises the need to expand the amount of reference data.

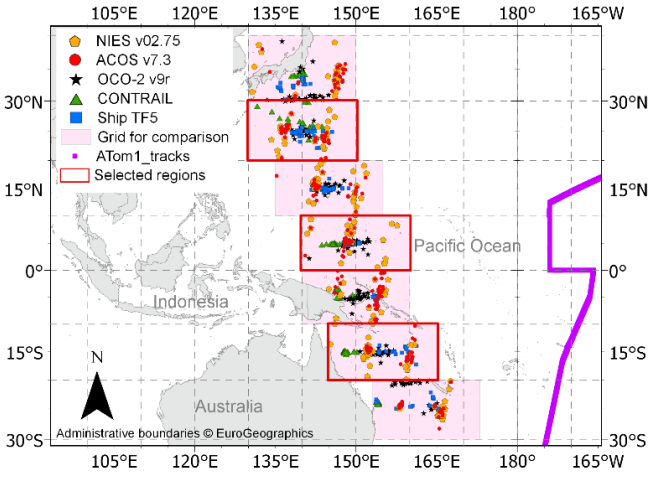

Figure R1. Comparison of the flight track of the Atom 1 campaign with the location of monthly averaged data of CO_2 from aircraft (CONTRAIL, green triangle), ship (Trans Future 5 - TF5, blue squares), the satellite retrievals from NIES (yellow diamonds), ACOS (red circles), and OCO-2 (black stars) between 2014 and 2017. Selected regions for the study within 10° latitude by 20° longitude boxes are shown in red frames. Administrative boundaries © EuroGeographics.

Comment

It would further strengthen the paper if you could extend the most southern box another 4 degrees to 34S, where you could show that the combined in situ + ACTM total column matches that from the (coastal) Wollongong TCCON station (filtering for onshore wind direction, perhaps).

Response

We agree that this would be beneficial and of wide interest. Unfortunately, south of the latitude 28° S, the aircraft data of CONTRAIL between Narita, Japan, and Sydney, Australia, are only obtained over land (Figure R2, green triangle). Hence, an overlap with ship data over the ocean area is not given. By using our methodology and combining ship data from the open ocean area with aircraft data over land, no realistic CO_2 profiles can be obtained. Therefore, we cannot extent the study area to 34° S at present.

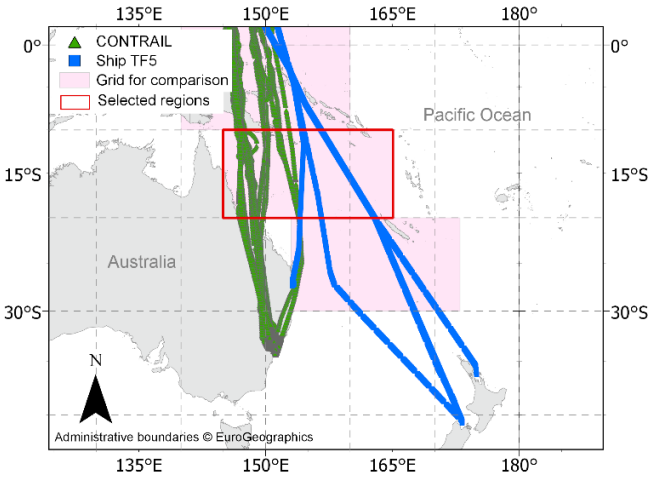

Figure R2. Location of the CO_2 data from aircraft (CONTRAIL, green triangle) and ship (Trans Future 5 - TF5, blue squares) between 2014 and 2017. Selected region for the study within 10° latitude by 20° longitude boxes is shown in the red frame. Administrative boundaries © EuroGeographics.

Comment

I found the Results and Discussion section confusing in places (see Specific comments for details) and difficult to follow.

Response

We revised the Results and Discussion section to clarify our statements. Please find our replies to the specific comments below.

Comment

Uncertainties are large in the differences and trends, and yet conclusions were drawn about whether satellite measurements agreed with the ship+CONTRAIL+ACTM-derived XCO2.

Response

We agree that the uncertainties of the differences between the observation-based XCO_2 (obs. XCO_2) and satellite XCO_2 shown in Table 3 and Fig. 5d-f of the manuscript are large, but significant in northern midlatitudes for ACOS (two-sided t-test, significance level α=0.05).

The difference in the trends between the satellite retrievals and the obs. XCO_2 is not significant at northern latitudes, but at the equator in case of ACOS and OCO-2 (two-sided t-test, significance level α=0.05, Table 4), they are significant. Although uncertainties are not small, the comparison of the obs. XCO_2 dataset with satellite retrievals gives important indications on how good the retrievals currently are, and if newly revised retrieval algorithm are improved towards minimizing the difference or not. Figure A1 of Appendix A of the manuscript, as well as Figure R3 below, which shows the obs. XCO_2 and the data of OCO-2 v9 versus OCO-2 v10, illustrate the applicability of our new observation-based XCO_2 dataset.

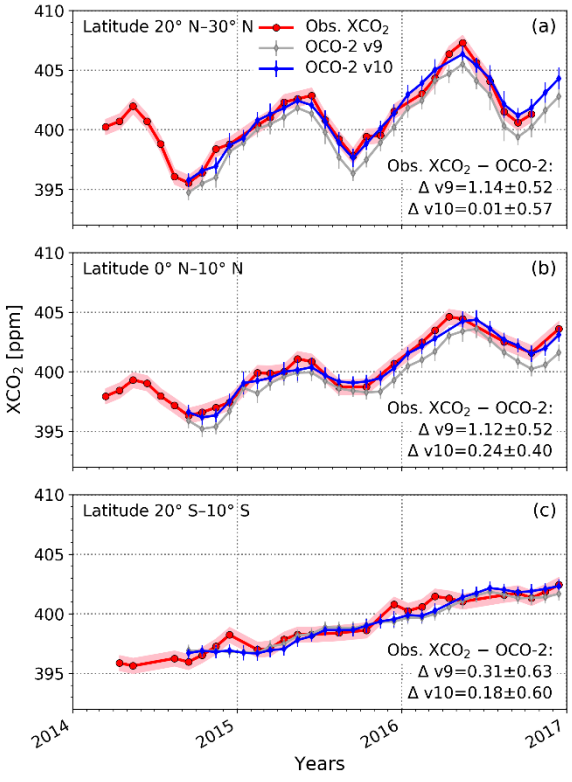

Figure R3. Comparison of the temporal variation of obs. XCO_2 (red) with XCO_2 derived from OCO-2 v9 (grey) and OCO-2 v10 (blue) for three selected latitude ranges. Red shaded areas are the uncertainty of the obs. XCO_2 which was obtained from the ±2 ppm variability in the observation-based CO_2 profile at ~850 hPa. Error bars show the standard deviation of the monthly averaged XCO_2.

For illustration, we added Figure R3 as Figure A2 to Appendix A of the revised manuscript as described below. The uncertainties connected with our dataset and the uncertainties of the comparison are clarified in the revised manuscript as follows:

Page 14, lines 321–323: *…and satellite XCO_2 in Figs. 5d-f.* ***The uncertainties of the obs. XCO_2 dataset are estimated to be 0.62 ± 0.01 ppm on average, which is derived from the ±2 ppm variation in the observation-based CO_2 profile at 2 km above sea level (section 3.2).***

Page 14, lines 330–334: *Agreement within 1 ppm on average is found in the SH (Figs. 5c and 5f).* ***The uncertainties of the differences between obs. XCO_2 and the satellite retrievals are large. However, the comparison indicates whether the results of the current satellite retrievals tend to show a systematic positive or negative offset (ACOS, OCO-2), or rather a random discrepancy. This comparison is of importance for revising the retrieval algorithm in future.***

Page 5, lines 139–141: ***Furthermore, OCO-2 version 10 was released.*** *An initial comparison between ACOS v7.3 and v9****, and between OCO-2 v9r and v10*** *is included in the* ***Appendix A (Figs. A1 and A2)*** *and section 5 Conclusions.*

Pages 19–20, lines 446–449: *An initial comparison of the* ***obs.*** *XCO_2 dataset with ACOS v9 revealed a decrease of the negative bias by more than 50%* ***on average*** *as compared to ACOS v7.3 (Fig. A1)****, and the comparison with OCO-2 v10, a decrease of the average bias by more than 90% as compared to OCO-2 v9r (Fig. A2).***

Specific comments

Comment

L38 – Why cite the 2018 value of atmospheric CO2? You could update this using the NOAA value for 2020.

Response

We revised the reference as follows:

Page 2, lines 36–39: *Since the beginning of the Industrial Era in the 1750s, fossil fuel combustion and other human activities have increased the atmospheric concentration of CO_2 from approximately 277 ppm to more than 4**10** ppm in 20**20** **(Dlugokencky, E. and Tans P.: Trends in Atmospheric Carbon Dioxide, NOAA/GML; www.esrl.noaa.gov/gmd/ccgg/trends/, last access: 7 January 2021).***

Page 27, lines 562–563: ***Dlugokencky, E. and Tans, P.: Trends in Atmospheric Carbon Dioxide, NOAA/GML; www.esrl.noaa.gov/gmd/ccgg/trends/, last access: 7 January 2021.***

Comment

L108 – Why do you only use the tropospheric data in your analyses? Wouldn't the lower stratospheric data provide important constraints on the total column and provide a check on the stratospheric model?

Response

First, the CONTRAIL flights rarely went into the lower stratosphere during our study period. Therefore, we could have filled out the lower part of the stratosphere with aircraft data only occasionally. For our methodology, we think it is better to have a consistently constrained stratosphere rather than using measurement data in a few profiles while most of the remaining profiles use the results of the MIROC4-ACTM only. Furthermore, the variation of CO_2 above the tropopause height varies much less than in the troposphere and can be successfully modelled (Figure R4).

Second, the aim of our study is not to provide a validation of the MIROC4-ACTM in the stratosphere, which is already one of best validated stratospheric models at present using high altitude balloon-borne measurements of SF_6 and CO_2-age-of-air (Patra et al., 2018).

We clarify the reason for excluding aircraft data of the stratosphere as follows:

Page 4, lines 111–114: *Only those data which were obtained below the tropopause height during the cruise at around 11 km altitude are used.* ***To define the tropopause height, we used the blended tropopause pressure (TROPPB), which is explained in detail in section 3.2. Data of the lower stratosphere were only occasionally obtained. We screened out those data in order to have a consistent methodology for constructing CO_2 profiles as explained in section 3.2.***

Comment

L125 – "By measuring the amount of light absorbed by CO2 and O2, the column average CO2 dry air mole fraction (XCO2) is estimated by taking ratio of the total column amounts of CO2 and O2, where O2 provides an estimate for the total column of dry air (Wunch et al., 2011)." This is true for TCCON, but I do not believe this is how the ACOS retrievals work. Please clarify.

Response

The Referee #1 is correct. Generally, XCO_2 quantifies the average mixing ratio of CO_2 in a column of dry air extending from the Earth's surface to the top of the atmosphere. It is derived by taking the ratio of the column integrated number densities of CO_2 and the total column of dry air. For the satellite retrievals, the total column of dry air is primarily derived from the surface pressure, which is mainly retrieved from the O_2 A-band in case of OCO-2, ACOS (O'Dell et al., 2012, 2018), and the GOSAT retrieval from NIES (Yoshida et al., 2011, 2013). Furthermore, the definitions of XCO_2 vary in how the dry air column is estimated and in how the vertical weighting is done (Crisp et al., 2012; O'Dell et al., 2012).

We revised the sentence as follows:

Page 5, lines 130–132: *By measuring the amount of light absorbed by CO_2 and O_2, the column average CO_2 dry air mole fraction (XCO_2) is estimated by taking ratio of the total column amounts of CO_2 and the total column of dry air* (**O'Dell et al., 2012, 2018;** Wunch et al., 2011; **Yoshida et al., 2011, 2013**).

Comment

Figure 2 – How does this profile compare with the GINPUT profile?

Response

Figure R4 shows the monthly averaged CO_2 profile calculated by ginput version 1.0.6 (purple line) in addition to the result of the MIROC4-ACTM and the observation-based CO_2 profile of Figure 2.

Especially in the lower troposphere, the ginput profile differs. This is explained by the fact that the TCCON prior do not try to capture the effect of emissions and do not ingest global flux datasets nor any longitudinal dependent behaviour. In contrast, the MIROC4-ACTM uses realistic flux and transport simulations and therefore, the ACTM derived profile is close to that derived from in situ measurements. In the stratosphere, the difference between the ACTM and ginput profile is small as compared to the troposphere.

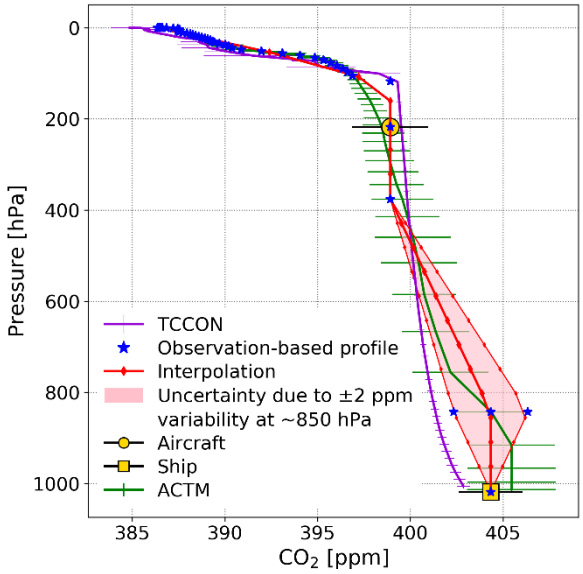

Figure R4. Comparison of the observation-based CO_2 profile (blue) with that obtained from the ACTM (green) and the TCCON a-priori profile of CO_2, calculated by ginput version 1.0.6 (purple). The example is obtained at the latitude 20° N–30° N, March 2014.

We clarify why we used the results of the ACTM instead of those from ginput in the response to the Referee's comment L172 below (Lines 207–231 of the response file).

Comment

If I understand correctly, the blue stars are a combination of model, in situ, and extrapolated data, is that correct? If so, calling it the "in situ" profile is misleading.

Response

The Referee #1 is correct, the blue stars are a combination of model, in situ, and extrapolated data. We intended to make it clear by using the terms "in situ constructed" in Figure 2 and "in situ adjusted profile" in the Figure caption. We revised the labelling in Figure 2, as well as in Figure A3 of Appendix A (Figure A4 of the revised manuscript) and the figure captions by using the term "observation-based profile". We also clarified the definition of the "observation-based profile" in the figure captions. Furthermore, we revised the naming of the resulting XCO_2 from "in situ XCO_2" to "observation-based XCO_2" (obs. XCO_2) throughout the whole the manuscript. Because the number of the occurrence of "in situ XCO_2" is large, we did not list each of the changes separately. The changes made are as follows:

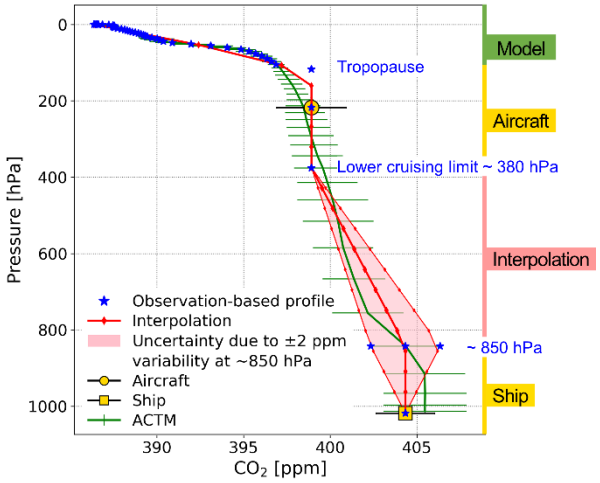

Page 8, lines 192–193: *Figure 2. Construction of the* ***observation-based*** *CO_2 profile (blue)* ***obtained*** *by using ship (SOOP) and aircraft (CONTRAIL) data (yellow) together with the results of the ACTM (green), and the interpolation (red). The example is obtained at the latitude 20° N–30° N, March 2014.*

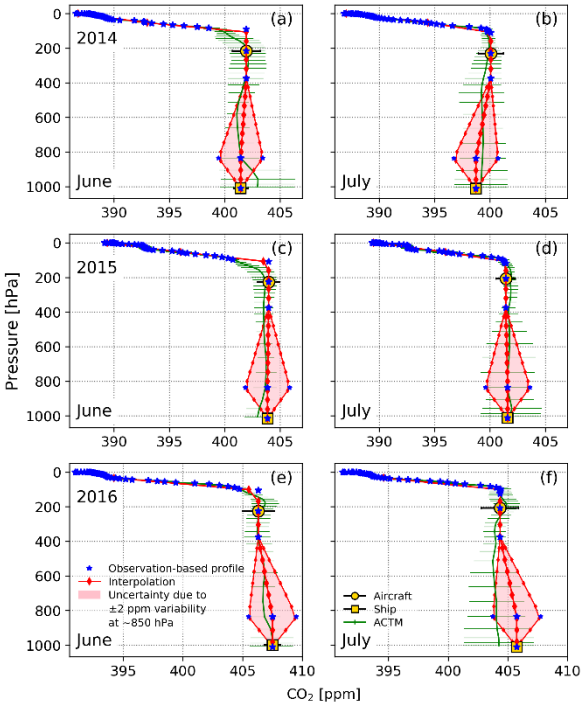

Page 24, lines 471–473: *Figure A4.* ***Observation-based*** *CO_2 profiles (blue)* ***obtained by*** *using ship (SOOP) and aircraft (CONTRAIL) data (yellow), together with the results of the ACTM (green), and the interpolation (red) for the month June and July in 2014 a), b), 2015 c), d), and 2016 e), f) at the latitude range 20° N–30° N.*

Lines 21, 30, 91, 169, 192, 205, 340, 364, 375, 428, 459-460: Changed from *in situ constructed/ in situ derived* to ***observation-based.***

Comment

L172 – Why use the MIROC-4 ACTM for the stratosphere instead of the GINPUT stratosphere? How do they compare?

Response

First, using the MIROC4-ACTM means that our method is fully independent of TCCON, which is important for using our methodology as complement for evaluating satellite retrievals. If TCCON and our method are independent, and satellite retrievals show a similar bias to both datasets, then the observed difference is a bias of the satellite data. In addition, the ginput prior is used in the OCO-2 v10. Therefore, having an independent stratosphere is a good cross check.

Second, the MIROC4-ACTM simulates the realistic CO_2 fluxes and transport processes as described above. Ginput starts from the average CO_2 mixing ratio measured at Mauna Loa and American Samoa and then imposes a latitudinally dependent seasonal cycle to derive the specific CO_2 profiles. Nevertheless, the CO_2 mixing ratios in the stratosphere are varying much less than in the troposphere and therefore, the results of the MIROC4-ACTM and ginput are similar as seen in Figure R4. We clarify the choice of the MIROC4-ACTM as follows:

Page 8, lines 195–199: *To account for the stratospheric partial column, we used results of the MIROC4-ACTM (Patra et al., 2018) above the TROPPB* ***(Fig. 2) instead of the results from ginput. First, by using the MIROC4-ACTM, our method is fully independent of TCCON, which is important for using our methodology as a complement to TCCON to evaluate satellite retrievals. Second, the MIROC4-ACTM uses realistic flux and transport simulations and is one of the best validated stratospheric models at present.***

Page 9, lines 215–217: *Second,* ***as mentioned earlier,*** *the MIROC4-ACTM is among the best validated stratospheric models* ***using high altitude balloon-borne measurements of SF_6 and CO_2-age-of-air*** *(Patra et al., 2018)****, and in the upper troposphere and lower stratosphere using CONTRAIL observations (Bisht et al., 2021)****.*

Page 26, lines 522–524: ***Bisht, J. S. H., Machida, T., Chandra, N., Tsuboi, K., Patra, P. K., Umezawa, T., Niwa, Y., Sawa, Y., Morimoto, S., Nakazawa, T., Saitoh, N. and Takigawa, M.: Seasonal Variations of SF_6, CO_2, CH_4, and N_2O in the***

UT/LS Region due to Emissions, Transport, and Chemistry, J. Geophys. Res. Atmos., 126(4), 1–18, doi:10.1029/2020JD033541, 2021.

Comment

L335 – "Hence, even though no assumption was necessary at that period, the negative bias persists (Fig. 5d, Fig. 6e), which indicates that the difference between in situ and satellite XCO2 can be linked to measurement uncertainties of the satellites." I do not follow this logic. Why couldn't the bias be caused by a bias in the ACTM stratosphere and not in the satellite retrievals?

Response

The variation of CO_2 in the stratosphere is much less as in the troposphere and can be simulated with high precision by the MIROC4-ACTM (Patra et al., 2018). Furthermore, as described in Lines 218–220 of the revised manuscript, our sensitivity test revealed that the error of the calculated XCO_2 due to the stratospheric part is only 0.2 ± 0.1 ppm on average. Based on the error induced by the stratosphere and the uncertainty derived from the variability in the observation-based CO_2 profile at ~850 hPa (0.62 ± 0.01 ppm), the largest reasonable bias is 0.9 ppm. This bias is not enough to explain the observed average negative discrepancy of 1.2 ± 0.4 ppm for ACOS and OCO-2 from June to September between 2014 and 2017.

We added the impact of the stratosphere as follows:

Page 16, lines 364–367: *Niwa et al. (2011) found similar straight vertical profiles between June and September in East Asia, based on aircraft observations and model results.* ***Furthermore, the maximum bias due to errors in the MIROC4-ACTM stratospheric CO_2 profile (0.9 ppm) is smaller than the average difference of 1.2 ± 0.4 ppm between the obs. XCO_2 and satellite observations of ACOS and OCO-2 between June and September (section 3.2).***

Comment

L353 – "The consistency with long-term studies support the correctness of the in situ XCO2, which implies that satellite XCO2 sometimes show a delayed response to CO2 changes." Again, I do not follow this argument. The satellites measure the total column in the atmosphere at the time of the measurement. Are you saying that the satellite measurements are wrong?

Response

As described in Lines 382–385 of the revised manuscript, long-term in situ measurements in the upper troposphere and at surface level report maxima and minima of CO_2 not later than May and September, while the satellite retrievals sometimes show the extreme values one month later. Based on the long-term in situ datasets, maxima in June and

minima in October are too late. We do not intend to say that the satellite measurements are wrong. Our observations suggest that these positive phase shifts of the satellite data are caused by remaining uncertainties which are introduced by limitations in the retrieval algorithm or the lack of validation data and therefore, have not been previously identified. The lack of validation data makes it difficult to characterize and correct these uncertainties. We know that from GOSAT and OCO-2 the retrieval algorithm to obtain XCO_2 from the measured radiance are undergoing rapid progress with almost one new version per year for OCO-2. We are hoping that the highly accurate ship and aircraft data over a unique geographical region will help us to build the capacity for the validation of satellite XCO_2 retrievals.
We clarify our statement as follows:

Page 17, lines 385–388: *The consistency with long-term studies support the correctness of the* ***obs.*** *XCO_2, which implies that satellite XCO_2 sometimes show a delayed response to CO_2 changes****, which might be caused by remaining uncertainties introduced by limitations in the retrieval algorithms and have not been previously identified due to the lack of validation data over the open ocean***

Comment
L359 – "In contrast, a significant increase of 3.84 ± 0.65 ppm yr−1 is observed by in situ XCO2 from 2015 to 2016, which is by _10% larger than that observed by satellites (3.39 ± 0.03)." Firstly, I don't see 3.39 ± 0.03 in Table 4 – is this a typo? Secondly, these numbers do not differ by 10% - their uncertainties overlap and therefore you cannot say anything conclusive about how they differ.

Response
On average, the increase of the mean values of all three satellite retrievals is 3.39 ± 0.03 ppm. That means, the value 3.39 ± 0.03 ppm is the average increase and its standard deviation of the mean values of all satellite retrievals in the period 2015 to 2016. We added a column to Table 4 with the average values as shown below.
The Referee #1 is correct that the uncertainties overlap. The difference in the increase of the obs. XCO_2 and that of the satellite XCO_2 is not significant at northern latitudes, but the increase of the obs. XCO_2 tends to be slightly higher. At the equator, the increase of the obs. XCO_2 is significantly higher than that of ACOS and OCO-2 (two-sided t-test, significance level α=0.05). We revised this part as follows:

Page 18, lines 392–396: *In contrast, a significant increase of 3.84 ± 0.65 ppm yr^{-1} is observed by* ***obs.*** *XCO_2 from 2015 to 2016.* ***The average increase of the mean values of all satellite retrievals is 3.39 ± 0.03 ppm yr^{-1}. This*** *rapid increase is also seen near the equator,* ***where the increase of the obs. XCO_2 is significantly higher than that of ACOS and OCO-2 (two-sided***

t-test, significance level α=0.05). S*imultaneously**, a larger negative bias of the satellite XCO_2 in 2016 as compared to the previous years* ***is observed*** *(Figs. 5b and 5e).*

Page 18, lines 398–401: ***Table 4.*** *Increase of XCO_2 between peaks of consecutive years and the standard error of the difference seen by* ***obs.*** *and satellite XCO_2 of GOSAT (NIES, ACOS) and OCO-2 between 2014 and 2017. Peak values are defined as mean of the three consecutive highest monthly averages during spring of each year. In 2016, the mean of ACOS and that of in situ XCO_2 at 0° N–10° N is based on 2 months due to limited data. "–" indicates missing data.* ***The right column shows the average increase of all satellite means and its standard deviation.***

	Obs. *XCO_2 (ppm yr^{-1})*	*NIES (ppm yr^{-1})*	*ACOS (ppm yr^{-1})*	*OCO-2 (ppm yr^{-1})*	***Avg. all satellites (ppm yr^{-1})***
			20° N–30° N		
2014–2015	*1.45 ± 0.63*	*1.42 ± 0.60*	*1.95 ± 0.54*	*–*	***1.68 ± 0.26***
2015–2016	*3.84 ± 0.65*	*3.37 ± 0.43*	*3.43 ± 0.40*	*3.36 ± 0.38*	***3.39 ± 0.03***
			0° N–10° N		
2014–2015	*1.72 ± 0.22*	*–*	*1.99 ± 0.30*	*–*	***–***
2015–2016	*3.87 ± 0.09*	*–*	*2.82 ± 0.37*	*3.52 ± 0.16*	***3.17 ± 0.35***

Technical comments

Comment

L55 – change "improves" to "improve"

Response

We revised the sentence as follows:

Page 2, lines 55–57: *These observations are most sensitive to the lower troposphere where CO_2 is most variable (Patra et al., 2003) and therefore, are able to improve the knowledge on local CO_2 emission and sinks (Connor et al., 2008).*

Comment

L56 – change "the second NASA" to "NASA's"

Response

We revised the sentence as follows:

Page 2, lines 58–60: *Japan's Greenhouse gases Observing Satellite (GOSAT), and the second NASA**'s** (National Aeronautics and Space Administration) Orbiting Carbon Observatory (OCO-2) are dedicated to inferring the concentration of GHGs from high-resolution spectra at NIR and SWIR wavelengths.*

Comment

L71 – TCCON has a very limited number of sites observing *the atmosphere over*open oceans. I'm not sure how you define this, since there are several coastal and island TCCON stations (e.g., Réunion Island, Ascension Island, Izaña, Burgos, Darwin, Wollongong) and the TCCON footprint is large enough that it would be sensitive to CO2 over oceans.

Response

The Referee #1 is correct that there are TCCON stations at coastal and island sites. However, wide areas over the open ocean, which we define as the area outside the coastal region, are not covered by TCCON stations as shown in Figure R5. Therefore, we speak of "very limited number". Even though the footprints of TCCON stations are large, reference data measured directly above open water areas provide a valuable complement to TCCON stations.

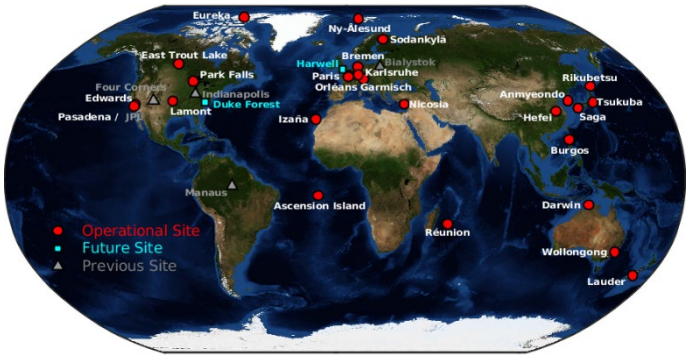

Figure R5. Location of current, future, and previous TCCON stations. Data are from 2/11/2020 (https://tccon-wiki.caltech.edu/Main/TCCONSites, 1/8/2021).

We clarified the definition of "the atmosphere over the open ocean" as follows:

Page 3, lines 73–74: However, TCCON **sites are land based and** very limited number of sites observe **the atmosphere over** open oceans**, which are defined as the ocean area outside the coastal region**.

Comments of Referee #2 and our responses to them

General comments

Comment

This manuscript details a new approach for evaluating variations of XCO2 over the Oceans by integrating ship, aircraft and model data to create an "in-situ based XCO2" dataset. This dataset is compared with GOSAT and OCO-2 satellite data to evaluate its capabilities. The paper does have value in its contribution to scientific progress and the scientific qualify of the work is good, however at points I think the paper needs to go into more detail of how and why specific parts of this method were done as I was left with several questions concerning this (as mentioned in my specific comments). The paper discusses biases between their in-situ XCO2 and the satellites, concluding that these can be attributed to measurement uncertainties of the satellite observations. I am left unconvinced by this argument and would like to see more analysis of other possible uncertainties in their in-situ profile to strengthen this claim (I explain in more detail in my specific comments no.11). The study goes on to look at differences in the seasonality of the satellite data vs the in-situ data, which again I am sceptical about because I was unconvinced that these differences aren't due to inaccuracies in the in-situ based columns.

Response

In the revised manuscript, we go into more detail of how and why we did specific parts of our methodology so that open questions are clarified. We also extended our analysis regarding the uncertainties of the observation-based profiles and considered these additional uncertainties for the comparison between observation-based XCO_2 (obs. XCO_2) and the satellite data. The details are explained under the specific comments below.

Specific comments

Comment

1. Page 3, line 71: I think it is misleading to say that TCCON has a very limited number of sites observing open oceans given that there are multiple sites on small islands in the oceans and multiple coastal sites. Again on line 80 you mention comparison to TCCON data in the tropical Pacific region. I think it would help to be more specific about these TCCON sites which are used and where they are.

Response

We agree with the Referee #2 that there are several coastal and island TCCON stations like Réunion Island, Ascension Island, Izaña, Burgos, Darwin, or Wollongong. This was also pointed out by Referee #1. As we replied to Referee #1, we wanted to emphasize that wide areas over the open ocean are not covered by TCCON stations. In the revised

manuscript, we define "open ocean" as the area outside the coastal region. We understand that the footprints of TCCON stations are large, but we think that reference data measured directly above open water areas provide a valuable complement to TCCON stations. Regarding the TCCON site mentioned in line 80, we refer to the station in Burgos at 19° N. Against XCO_2 data of this station, data of OCO-2 v8 have a bias of −0.7 ppm (Kulawik et al., 2019). We clarified these points in the revised manuscript as follows:

Page 3, lines 73–74: *However, TCCON* ***sites are land based and*** *very limited number of sites observ****e the atmosphere over*** *open oceans****, which are defined as the ocean area outside the coastal region****.*

Page 3, lines 81–83: *More recent comparisons of OCO-2 XCO_2 estimates to in situ measurements from the NASA Atmospheric Tomography Mission reveals a systematic bias of −0.7 ppm over the tropical Pacific, that is also seen in* ***the*** *data* ***at Burgos, a TCCON station*** *in that region* (**Kulawik et al., 2019; Velazco et al., 2017**).

Page 28, lines 598–602: ***Kulawik, S. S., Crowell, S., Baker, D., Liu, J., Mckain, K., Sweeney, C., Biraud, S. C., Wofsy, S., Dell, C. W. O., Wennberg, P. O., Wunch, D., Roehl, M., Deutscher, N. M., Kiel, M., Griffith, D. W. T., Velazco, V. A., Dubey, M. K., Sepulveda, E., Elena, O., Rodriguez, G., Té, Y., Heikkinen, P., Dlugokencky, E. J., Gunson, M. R., Eldering, A., Fisher, B. and Osterman, G. B.: Characterization of OCO-2 and ACOS-GOSAT biases and errors for CO_2 flux estimates, (October), 2019.***

Page 30, lines 678–680: ***Velazco, V. A., Morino, I., Uchino, O., Hori, A., Kiel, M., Bukosa, B., Deutscher, N. M., Sakai, T., Nagai, T., Bagtasa, G., Izumi, T., Yoshida, Y. and Griffith, D. W. T.: TCCON Philippines: First measurement results, satellite data and model comparisons in Southeast Asia, Remote Sens., 9(12), 1–18, doi:10.3390/rs9121228, 2017.***

Comment

2. Page 3, line 72: Can you please clarify if this is an ocean bias or if this bias is for land and ocean combined at these sites.

Response

It is an ocean bias. It is the average bias between GOSAT ocean H-Gain soundings and the TCCON stations Bremen, Saga, Burgos, Darwin, and Reunion. We clarified our statement as follows:

Page 3, lines 74–75: *Between the GOSAT NIES* ***soundings over the ocean*** *and TCCON sites near the ocean, a bias of −1.09 ± 2.27 ppm was found (Morino et al., 2020).*

Comment

3. Page 4, lines 102-104: The last part of this sentence doesn't make sense to me "if the standard deviation does not exceed 3 ppm".

Response

We clarified the sentence as follows:

Page 4, lines 105– 108: *Forty seconds (s) after the switch from standard gas to air sample, data are collected as averages of 10 s during the ascent and decent, and 1 min averages during the cruise (~ 15 km horizontal distance)**. Data of each 10 s and 1 min period are rejected** if the standard deviation exceed**s** 3 ppm (Umezawa et al., 2018).*

Comment

4. Page 4, line 108: Please could you explain how you determined the tropopause height that you use as a cut off for the aircraft data. Did you use a static 11 km for all measurements or did you calculate it for each time and location?

Response

We used the blended tropopause pressure (TROPPB) as cut off for the aircraft data. The TROPPB was extracted from GEOS-FP (Goddard Earth Observing System – forward processing) meteorology data using the python suite "ginput" version 1.0.6 (Laughner et al., 2021). It was calculated for every 3 hours (00, 03, 06, 09, 12, 15, 18, 21 o'clock UTC) for the 5th, 15th, and 25th of each month at each centre location of the 10° latitude by 20° longitude grid.

We added the explanation on how we determined the tropopause height as follows:

Page 4, lines 111–114: *Only those data which were obtained below the tropopause height during the cruise at around 11 km altitude are used. **To define the tropopause height, we used the blended tropopause pressure (TROPPB), which is explained in detail in section 3.2. Data of the lower stratosphere were only occasionally obtained. We screened out those data in order to have a consistent methodology for constructing CO_2 profiles as explained in section 3.2.***

Page 7, lines 181–188: ***The TROPPB** is defined as a combination of a thermal tropopause- and dynamic tropopause pressure (Wilcox et al., 2012). The TROPPB data are extracted from GEOS-FP (Goddard Earth Observing System – forward processing) meteorology data using the python suite "ginput" **version 1.0.6** **(Laughner et al., 2021)**. Ginput was developed to generate a priori vertical mixing ratios of chemical species (e.g., CO_2, CO, CH_4, N_2O) for the open source TCCON retrieval algorithm, GGG2020 (Laughner et al., in prep). **The TROPPB was calculated every 3 hours on the 5th, 15th, and 25th of each***

month for each centre location of the 10° latitude by 20° longitude boxes. Between 2014 and 2017, the highest monthly variation was found at 20° N–30° N with a standard deviation ranging from 0 to 24 hPa (0.02 to 23.77 hPa) and an average standard deviation of 10 ± 5 hPa. The maximum difference of 24 hPa at the level of the TROPPB corresponds to difference in the altitude of 1 to 2 km.

Page 28, lines 606–607: ***Laughner, J., Andrews, A., Roche, S., Kiel, M. and Toon, G.: ginput v1.0.7b: GGG2020 prior profile software, CaltechDATA., 2021.***

Comment

5. Page 4, methodology: Why did you settle on monthly resolution? I am interested if instead of comparing with monthly averages it would have been possible to compare any of the in-situ data more directly to satellite overpasses on the same day for example. Were there any cases where you were able to do this or were the ship, aircraft and satellite data never on the same day?

Response

There were daily coincidences of satellite, aircraft, and ship data. However, the number was limited. Because our primary focus was to analyse the seasonal, interannual and latitudinal variation of XCO_2, we decided to settle on monthly resolution in the current study.

We clarified why we used a monthly resolution in the revised manuscript as follows:

Page 6, lines 160–161: ***For the analysis of the seasonal and interannual variation of CO_2, we chose the*** *monthly averages of the satellite, in situ, and model datasets.*

Comment

6. Page 6, comments on section 3.2 and Figure 2: Naming this constructed profile "in-situ" when it consists of both in-situ and model data is misleading.

Response

We agree that the naming is misleading. Referee #1 criticised the same point. We revised the labelling in Figure 2, as well as in Figure A3 of Appendix A (Figure A4 of the revised manuscript) and the figure captions by using the term "observation-based" profile. We also clarified the definition of the "observation-based profile" in the figure captions. Furthermore, we revised the naming of the resulting XCO_2 from "in situ XCO_2" to "observation-based XCO_2" (obs.

XCO_2) throughout the whole manuscript. Because the number of the occurrence of "in situ XCO_2" is large, we did not list each of the changes separately. The changes made are as follows:

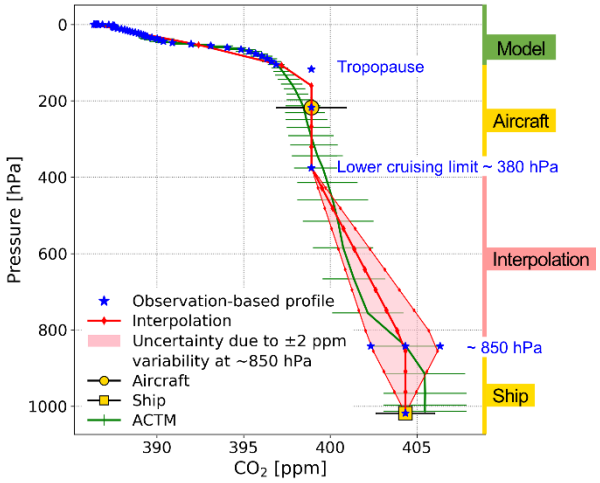

Page 8, lines 192–193: *Figure 2. Construction of the* ***observation-based*** *CO_2 profile (blue)* ***obtained*** *by using ship (SOOP) and aircraft (CONTRAIL) data (yellow) together with the results of the ACTM (green), and the interpolation (red). The example is obtained at the latitude 20° N–30° N, March 2014.*

Lines 21, 30, 91, 169, 192, 205, 340, 364, 375, 428, 459-460: Changed from *in situ constructed/ in situ derived* to ***observation-based.***

Comment

7. Page 6, comments on section 3.2 and Figure 2: Please could you comment in more detail why you chose to extrapolate the ship concentrations up to 850 hpa.

Response

We assumed that the impact of the CO_2 measured at sea level reaches up to about 850 hPa. This corresponds to the 3rd and 4th pressure level of the GOSAT NIES and ACOS retrieval, counted from the surface. It represents the boundary layer in which most of the rather rapid changes in the CO_2 mixing ratio occur according to previous studies of Frankenberg et al. (2016) and Inai et al. (2018). At pressure levels above, the CO_2 mixing ratios are rather stable or keep changing linearly up to about the tropopause height (Frankenberg et al., 2016; Inai et al., 2018).

We clarified why we extrapolate the ship data up to ~850 hPa as follows:

Pages 6–7 , lines 171–177: *Ship data are extrapolated vertically to ~850 hPa**, which corresponds to the 3rd and 4th pressure level of NIES and ACOS, respectively, counted from the surface**. We chose this cut off as it represents the boundary layer above sea level in which most of the rapid variation of CO_2 occur**. Previous balloon and aircraft measurements by the HIPPO campaign over the Tropical Eastern and Western Pacific showed **stronger** CO_2 variation of **about** 1 to 2 ppm within the first 2 km above sea level. **Above this level, the CO_2 mixing ratios were rather stable or kept changing linearly up to about the tropopause height** (Frankenberg et al., 2016; Inai et al., 2018). To account for that variation **within the boundary layer**, we added a ±2 ppm uncertainty to the CO_2 estimates **at ~850 hPa**.*

Comment

8. Page 6, comments on section 3.2 and Figure 2: You say that you extrapolate the aircraft data down to 380 or 400 hpa; and then say that the tropopause pressure is used as upper limit for the extrapolation. So are you also extrapolating the data upwards to the tropopause or is this only the case when the aircraft data are above the tropopause?

Response

We are also extrapolating the aircraft data upwards to the height of the blended tropopause pressure. Aircraft data above the tropopause were excluded before the analysis in order to have a consistent stratosphere as explained in our response to Referee #1 in Lines 126–129 of the response file. Similarly, Ohyama et al. (2020) extrapolated profile data obtained by an aircraft upwards to the tropopause height at the TCCON site Burgos.

We clarified our explanation as follows:

Page 7, lines 177–180: *Aircraft data from the cruise portion of the flight, which is usually between 380 and 200 hPa, are selected. These aircraft data are extrapolated down to the lower cruising height limit at 380 hPa, and at 30° N–40° N at 400 hPa. **Furthermore, the aircraft data is also extrapolated upwards to the** blended tropopause pressure (TROPPB).*

Comment

9. Page 6, comments on section 3.2 and Figure 2: The vertical grid which you are interpolating onto is not discussed. It is clear from Figure 2 that your red interpolation line does not have the vertical resolution of the different components which you are using to make the "in-situ" profile. I know that you have done this to match the profile of the satellite retrievals, but you don't explain this. ACOS GOSAT and OCO-2 soundings have a different pressure profile for every sounding because they are built from the surface pressure which does change between soundings. Did you calculate the "in-situ" XCO2 for each satellite sounding separately and then average the monthly/spatial results. Or did you assume one fixed (or perhaps make your own average) profile for pressure, apriori co2 and the averaging kernel?

Response

Thank you for pointing out our missing explanation of the grid used for the interpolation. In order to compare the calculated XCO_2 based on the observation-based profile with that from the satellite soundings, we did the following. We interpolated the observation-based profiles based on the monthly averaged data on the corresponding monthly averaged pressure grid of the ACOS retrieval for the time period 2014 to May 2016. After that date, we used the monthly averaged pressure grid of NIES due to the temporal limit of the ACOS v7.3 product as also explained in Lines 210–212 of the revised manuscript.

We added the explanation of the grid used as follows:

Page 8, lines 200–202: *To calculate the XCO_2 that the satellite would have seen given the CO_2 profile constructed from in situ data,* ***we first interpolate these profiles onto the corresponding monthly averaged pressure grid of the ACOS and NIES retrievals, then*** *we use Eq. (15) of Connor et al. (2008):*

Page 9, lines 210–212: *Because the ACOS retrieval provides a higher number of valid data, we used the* ***pressure levels and*** *parameters from ACOS as representative for the calculation. After May 2016, we use the* ***pressure grid and*** *parameters from NIES due to the temporal limit of the ACOS v7.3 product.*

Comment

10. Page 8, line 215: You say that the values you get are similar to Matsueda et al. 2008. Can you be more specific on how similar they are? You do this afterwards with the Conway et al. 1994 numbers so it would paint a more complete picture if you could also give numbers in this instance.

Response

At 20° N –30° N, we found a peak-to-trough amplitudes of 6.5 ± 0.6 ppm in the upper troposphere which decreased to about 4 ppm at the equator (Lines 230–232 of the revised manuscript). Matsueda et al. (2008) found a decrease from 6 ppm at 30° N to 3 ppm at the equator. Our sentence in the manuscript was misleading as the numbers in the brackets correspond to the observations made by Matsueda et al. (2008).

We revised the sentence as follows:

Pages 9–10, lines 234–239: *Seasonal cycles and decreasing amplitudes* ***in the upper troposphere*** *from North to South (7 ppm to* ***4*** *ppm) are similar to that observed by Matsueda et al. (2008).* ***They found a decrease from 6 ppm at 30° N to 3 ppm at the***

equator *over the same region between 2005 to 2007 using aircraft based flask samples. At sea level, seasonal cycle amplitudes that decrease from about 8 ppm at 20° N–30° N to 3 ppm at the equator were reported by the global sampling network of the National Oceanic and Atmospheric Administration's Climate Monitoring and Diagnostics Laboratory (NOAA/CMDL) (Conway et al., 1994).*

Comment

11. I disagree with your assessment that the mid troposphere is the only uncertainty in the in-situ profile which you need to consider. You also should consider the tropopause height as well. We can see from Figure A3 that the interpolated profile deviates from the model profile at the tropopause in panels a and c. I think your concentrations at the tropopause can't be overlooked as an uncertainty because the ACTM and your in-situ profile are clearly in disagreement over the location of the tropopause in some of these figures. It may be that the satellite data and your in-situ XCO2 are different because your tropopause height is incorrect, which would lead to seasonally dependent biases. How much does your tropopause height vary over all of the measurement times and locations in a month? By how much will this change your XCO2 values and can this account for the differences you see to the satellite data?

Response

We thank Referee #2 for pointing out the uncertainty due to the tropopause height. It is correct that the variation of the tropopause height impacts the obs. XCO_2 and should be considered. Our results show that the data of the monthly averaged TROPPB over the ocean (see our reply to comment 4, Lines 415–438 of the response file) have the highest variation at northern midlatitudes (20° N–30° N). The standard deviation ranged from 0 to 24 hPa (0.02 to 23.77 hPa) with an average of 10 ± 5 hPa. At 0° N–10° N and 20° S–10° S, the standard deviations are lower, which ranged from 6 to 11 hPa (average 8 ± 1 hPa), and from 4 to 12 hPa (average 7 ± 2 hPa), respectively (Table R1).

Table R1. Range of the standard deviation (Std.) of the monthly averaged TROPPB (left column), and average standard deviation of all month (right column) in hectopascal (hPa) at each 10° latitude by 20° longitude box.

	Std. range (hPa)	Average std. (hPa)
20° N–30° N	0 – 24	10 ± 5
0° N–10° N	6 – 11	8 ± 1
20° S–10° S	4 – 12	7 ± 2

To test the effect of the TROPPB on the calculated XCO_2, we assumed the highest average variation of 15 hPa found at 20° N–30° N over the ocean (average standard deviation of 10 ± 5 hPa).

Based on observation-based CO_2 profiles with a TROPPB ±15 hPa, we calculated the corresponding XCO_2 and compared the results with our previous calculated obs. XCO_2. The total average difference in the obs. XCO_2 is only

0.03 ± 0.06 ppm for the time period 2014 to 2017 at 20° N–30° N. Considering both the uncertainty of the TROPPB and that uncertainty caused by the variability of 2 ppm at 850 hPa in the observation-based profile (0.62 ± 0.01 ppm on average), the largest reasonable uncertainty is 0.72 ppm.

In comparison, the observed average difference between the obs. XCO_2 and satellite observations of ACOS v7.3 and OCO-2 v9 is 1.2 ± 0.4 ppm between June and September in 2014 to 2017. That means, even if we consider the maximal possible uncertainty of the obs. XCO_2 with 0.7 ppm, the discrepancy to ACOS v7.3 and OCO-2 v9 cannot be fully explained. On the other hand, the comparison of the obs. XCO_2 with the newer satellite retrievals ACOS v9 and OCO-2 v10 shows a reduced difference. This suggests that some bias has its origin in the older retrieval algorithm which is reduced in the newer versions (Figure A1 and A2 of the revised manuscript).

Furthermore, the sensitivity analysis, described in Lines 218–220 of the revised manuscript, showed that the impact of the upper troposphere, including the TROPPB, and stratosphere on the XCO_2 is only 0.2 ± 0.1 ppm on average.

To clarify the uncertainty of the obs. XCO_2, we revised the text as follows:

Page 16, lines 350–361: *It reveals that generally, the largest differences in the NH coincide with the latitude of the monthly XCO_2 maxima. Namely, at 30° N–40° N in spring and autumn with up to 3 ppm (between* ***obs.*** *XCO_2 and ACOS in March) (Figs. 6a and 6d) and in June at 10° N–20° N with a discrepancy of up to 2 ppm (between* ***obs.*** *XCO_2 and OCO-2) (Figs. 6b and 6e).* ***The difference might be caused by uncertainties in the obs. XCO_2 due to the variability of the TROPPB (section 3.2). However, the uncertainty in the TROPPB results in a difference in the obs. XCO_2 of only 0.03 ± 0.06 ppm on average. This leads to a total estimated error of 0.7 ppm considering the uncertainty of 0.62 ± 0.01 ppm derived from the ±2 ppm variation in the observation-based CO_2 profile at 2 km above sea level (section 3.2). It is known that a****tmospheric CO_2 mixing ratios in midlatitudes are characterized by high spatiotemporal variability. Therefore, the observed discrepancies in the NH may arise from differences in sample numbers, location and time within each month and latitude-longitude range. In particular, the largest uncertainty in the obs. XCO_2 likely results from the constructed CO_2 profile in the mid-troposphere, as no observational constraints are available for that part of the atmosphere and simply a linear interpolation between the ship and aircraft data was assumed (section 3.2).*

Page 16, lines 364–367: *Niwa et al. (2011) found similar straight vertical profiles between June and September in East Asia, based on aircraft observations and model results.* ***Furthermore, the maximum bias due to errors in the MIROC4-ACTM stratospheric CO_2 profile (0.9 ppm) is smaller than the average difference of 1.2 ± 0.4 ppm between the obs. XCO_2 and satellite observations of ACOS and OCO-2 between June and September (section 3.2).***

Page 7, lines 181–188: ***The TROPPB*** *is defined as a combination of a thermal tropopause- and dynamic tropopause pressure (Wilcox et al., 2012). The TROPPB data are extracted from GEOS-FP (Goddard Earth Observing System – forward*

processing) meteorology data using the python suite "ginput" ***version 1.0.6*** **(Laughner et al., 2021)**. *Ginput was developed to generate a priori vertical mixing ratios of chemical species (e.g., CO_2, CO, CH_4, N_2O) for the open source TCCON retrieval algorithm, GGG2020 (Laughner et al., in prep).* ***The TROPPB was calculated every 3 hours on the 5th, 15th, and 25th of each month for each centre location of the 10° latitude by 20° longitude boxes. Between 2014 and 2017, the highest monthly variation was found at 20° N–30° N with a standard deviation ranging from 0 to 24 hPa (0.02 to 23.77 hPa) and an average standard deviation of 10 ± 5 hPa. The maximum difference of 24 hPa at the level of the TROPPB corresponds to difference in the altitude of 1 to 2 km.***

Comment

12. I would be interested to see how the ACTM XCO2 would look if you interpolated it onto the satellite grid in the same way you have done for your in-situ data, and how this would compare with both the satellite and in-situ XCO2.

Response

Referring to Figure A3 (Figure A4 of the revised manuscript) as mentioned in comment 11, we interpolated the monthly averaged ACTM CO_2 profiles onto the 20 pressure levels of GOSAT ACOS for June and July 2014 and 2015, and for June and July 2016 onto the 15 pressure levels of GOSAT NIES. At 20° N–30° N, the variation of the monthly averaged ACTM CO_2 data varies from 0.6 % (2.4 ppm) at surface level to less than 0.02% (0.07 ppm) at the upper troposphere from 2014 to 2017. We assumed an average variation of 0.3% at each of the 67 pressure layers of the ACTM. The comparison of the ACTM CO_2 profile with that interpolated on the ACOS grid shows mainly differences in the upper troposphere which is explained by the lower resolution of the ACOS grid (Fig. R6 and Fig. R7).

The resulting XCO_2 is within 1 ppm (average difference 0.20 ± 0.32 ppm) of that of the obs. XCO_2. The highest average difference to the satellite retrievals occur for ACOS and OCO-2 with 1.11 ± 0.28 ppm and 1.02 ± 0.40 ppm, respectively (Table R2 and R3). The results reveal that XCO_2 based on the ACTM show a similar difference to XCO_2 from ACOS and OCO-2 as the obs. XCO_2 (compare Table 3 in the revised manuscript).

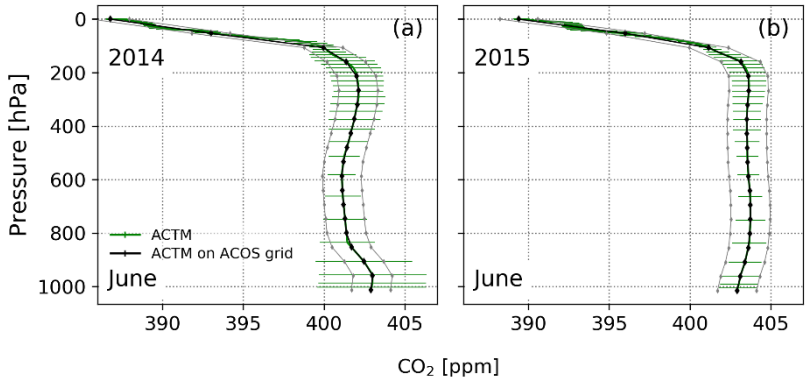

Figure. R6. Comparison of the CO_2 profiles of the ACTM (green) with that interpolated onto the 20 pressure levels of ACOS (black). Error bars are the standard deviation of the monthly averages of the ACTM. Grey lines represent 0.3% uncertainty of the interpolated ACTM.

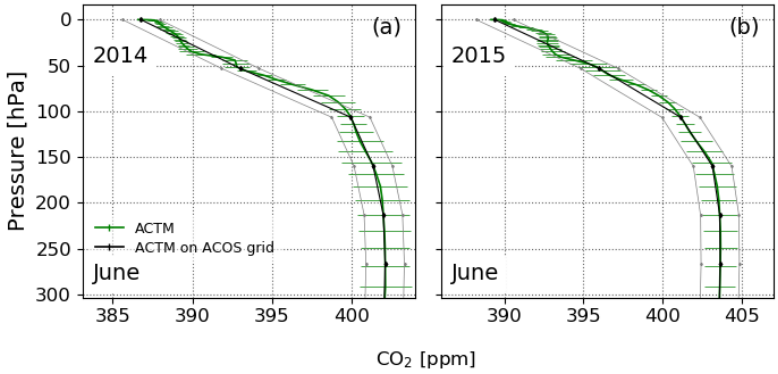

Figure. R7. Similar to Fig. R6, but with the y-limits set to focus on the upper troposphere. Comparison of the CO_2 profiles of the ACTM (green) with that interpolated onto the 20 pressure levels of ACOS (black). Error bars are the standard deviation of the monthly averages of the ACTM. Grey lines represent 0.3% uncertainty of the interpolated ACTM.

Table R2. The monthly averaged (Avg.) values and its standard deviation of ACTM based XCO_2, obs. XCO_2 and satellite XCO_2 of GOSAT (ACOS, NIES) and OCO-2 in the latitude range 20° N–30° N, for June and July, 2014–2017.

Date (MM/YY)	Avg. ACTM XCO_2 (ppm)	Avg. obs. XCO_2 (ppm)	Avg. ACOS (ppm)	Avg. NIES (ppm)	Avg. OCO-2 (ppm)
6/14	400.65 ± 1.07	400.7 ± 0.62	399.78 ± 1.24	401.49 ± 1.64	–
7/14	398.79 ± 1.06	398.8 ± 0.63	397.93 ± 1.12	399.57 ± 0.7	–
6/15	402.47 ± 1.08	402.87 ± 0.63	401.34 ± 1.20	402.67 ± 0.71	401.35 ± 0.69
7/15	401.01 ± 1.06	400.82 ± 0.62	399.45 ± 1.20	401.06 ± 1.39	399.78 ± 0.97
6/16	405.48 ± 1.10	405.62 ± 0.63	–	405.49 ± 0.96	404.1 ± 0.69
7/16	403.26 ± 1.12	404.06 ± 0.63	–	401.85 ± 3.74	402.91 ± 1.28

Table R3. Difference between the average values of ACTM based XCO_2 and the obs. XCO_2 and satellite XCO_2.

Date (MM/YY)	ACTM − in situ XCO_2 (ppm)	ACTM − ACOS XCO_2 (ppm)	ACTM – OCO2 XCO_2 (ppm)	ACTM − NIES XCO_2 (ppm)
6/14	−0.05	0.87	–	−0.84
7/14	−0.01	0.86	–	−0.78
6/15	−0.4	1.10	1.1	−0.2
7/15	0.2	1.60	1.2	−0.1
6/16	−0.14	–	1.38	−0.01
7/16	−0.8	–	0.35	1.41

Comment

13. Page 15, line 354: It is unclear to me how satellite XCO2 can show a delayed response to CO2 changes since it is measuring in real time. Please could you elaborate on this.

Response

We agree, the argument needs to be clarified. Referee #1 criticized the same point. What we observed is that the satellite retrievals sometimes show the extreme values of XCO_2 delayed by one month as compared to our obs. XCO_2 dataset. We know from previous long-term in situ measurements in the upper troposphere and at surface level (Lines 382–385 of the revised manuscript) that maxima and minima of CO_2 occur not later than May and September, respectively. Therefore, maxima in June and minima in October of the satellite retrievals are later than observed by the in situ measurements.

Satellite XCO_2 is measured in real time. We argue that there are remaining uncertainties which are introduced by limitations in the retrieval algorithm, which have not been previously identified due to the lack of validation data over the open ocean. We know that from GOSAT and OCO-2 the retrieval algorithm to obtain XCO_2 from the measured radiance are undergoing rapid progress with almost one new version per year for OCO-2. We are hoping that the highly accurate ship and aircraft data over a unique geographical region will help us to build the capacity for the validation and improvement of satellite XCO_2 retrievals.

We clarified our statement as follows:

Page 17, lines 385–388: *The consistency with long-term studies support the correctness of the* ***obs.*** *XCO_2, which implies that satellite XCO_2 sometimes show a delayed response to CO_2 changes****, which might be caused by remaining uncertainties introduced by limitations in the retrieval algorithms and have not been previously identified due to the lack of validation data over the open ocean.***

Page 19, lines 441–444: *Hence, the result indicates that even if the retrievals complement each other, measurement uncertainties remain, which limit the accurate interpretation of spatiotemporal changes in CO_2 fluxes by satellites alone.* ***These uncertainties might be introduced by limitations in the retrieval algorithms and have not been previously identified due to the lack of validation data over the open ocean.***

Comment

14. Page 16, line 359: Please add the uncertainty and be more accurate in your "less than 2ppm" number since you are being very precise with the number you are comparing it to in the next sentence.

Response

We revised the sentence as follows:

Page 18, lines 391–392: *From 2014 to 2015,* ***obs.*** *and satellite XCO_2 increased by* ***1.61 ± 0.24 ppm yr^{-1} on average*** *at 20° N–30° N (****Table 4,*** *Fig. 5a).*

Comment

15. Page 16, line 360: 3.84 0.65 and 3.39 0.03 overlap so you can't draw conclusions about their difference.

Response

Referee #2 is correct that the uncertainties overlap. This was also pointed out by Referee #1. The difference in the increase of the obs. XCO_2 and that of the satellite XCO_2 isn't significant at northern latitudes, but the increase of the obs. XCO_2 tends to be slightly higher. At the equator, the increase of the obs. XCO_2 is significantly higher than that of ACOS and OCO-2 (two-sided t-test, significance level α=0.05). We revised this part as follows:

Page 18, lines 392–396: *In contrast, a significant increase of 3.84 ± 0.65 ppm yr^{-1} is observed by* ***obs.*** *XCO_2 from 2015 to 2016.* ***The average increase of the mean values of all satellite retrievals is 3.39 ± 0.03 ppm*** *yr^{-1}****. This*** *rapid increase is also seen near the equator,* ***where the increase of the obs. XCO_2 is significantly higher than that of ACOS and OCO-2 (two-sided t-test, significance level α=0.05). S****imultaneously****, a larger negative bias of the satellite XCO_2 in 2016 as compared to the previous years* ***is observed*** *(Figs. 5b and 5e).*

Comment

16. You conclude by saying that datasets such as yours can augment TCCON data. Did you consider applying your method to other aircraft and ground data at TCCON sites to compare with TCCON itself?

Response

In future, we plan to extend the temporal coverage, and increase the temporal and spatial resolution. Then we can also compare our method to other aircraft and also to ground data from TCCON stations to strengthen our results. Currently, we couldn't compare our data with other aircraft campaign such as CO_2 profiles from HIPPO (Hiaper Pole-to-Pole Observations) or ATom (Atmospheric Tomography Mission). This is because no coincident data between the years 2014 and 2017 in the longitude–latitude range of 130° E to 173° E and 30° S to 40°N exist. It would be beneficial to compare our results with data of coastal or island TCCON stations to test our methodology. But again, a direct comparison is currently not possible as no co-located CONTRAIL (aircraft) and ship measurements with TCCON stations are available. For example, for the latitude range of the TCCON station Wollongong, we don't have aircraft data from over the ocean (compare our response to Referee#1, Lines 31–44 of the response file).

Our immediate plan is to compare our results with ship based EM27/Sun Fourier Transform infrared spectrometer measurements, which were conducted this spring on the research vessel Mirai in collaboration with the research group of André Butz of the University of Heidelberg.

Technical corrections

Comment

Page 2, line 45: You say that most sites are in North America and Europe, and some are in East Asia and Oceania. This reads as though there are no sites in the other continents, which I don't think was your intention to say. Please reword this sentence.

Response

We revised the sentence as follows:

Page 2, lines 46–48: *There are now more than 100 surface measurement sites around the globe, but most are located on land in North America and Europe, and some in the East Asia and Oceania**, and few in other continents** (e.g., Crowell et al., 2019; Hakkarainen et al., 2019).*

Comment

Page 2, line 55: "improves" should be "improve".

Response

The sentence is corrected as follows:

Page 2, lines 55–57: *These observations are most sensitive to the lower troposphere where CO_2 is most variable (Patra et al., 2003) and therefore, are able to improve the knowledge on local CO_2 emission and sinks (Connor et al., 2008).*

Comment

Page 3, line 74: "Aircrafts" should be "aircraft".

Response

The sentence is corrected as follows:

Page 3, lines 76–78: *In combination with surface measurements, vertical profiles of CO_2 obtained by aircraft can constrain XCO_2 but are very limited (e.g., Frankenberg et al., 2016; Inoue et al., 2013; Wofsy, 2011; Wofsy et al., 2018).*

Comment

Page 3, line 79: Negative symbol isn't the same type of symbol used in previous cases.

Response

The sentence is corrected as follows:

Page 3, lines 81–83: *More recent comparisons of OCO-2 XCO_2 estimates to in situ measurements from the NASA Atmospheric Tomography Mission reveals a systematic bias of −0.7 ppm over the tropical Pacific, that is also seen in* ***the*** *data* ***at Burgos, a TCCON station*** *in that region* ***(Kulawik et al., 2019; Velazco et al., 2017).***

Comment

Page 3, line 80: Remove journal and doi from citation.

Response

The sentence is corrected as follows:

Page 3, lines 81–83: *More recent comparisons of OCO-2 XCO_2 estimates to in situ measurements from the NASA Atmospheric Tomography Mission reveals a systematic bias of −0.7 ppm over the tropical Pacific, that is also seen in* ***the*** *data* ***at Burgos, a TCCON station*** *in that region* ***(Kulawik et al., 2019; Velazco et al., 2017).***

Page 28, lines 598–602: ***Kulawik, S. S., Crowell, S., Baker, D., Liu, J., Mckain, K., Sweeney, C., Biraud, S. C., Wofsy, S., Dell, C. W. O., Wennberg, P. O., Wunch, D., Roehl, M., Deutscher, N. M., Kiel, M., Griffith, D. W. T., Velazco, V. A., Dubey, M. K., Sepulveda, E., Elena, O., Rodriguez, G., Té, Y., Heikkinen, P., Dlugokencky, E. J., Gunson, M. R., Eldering, A., Fisher, B. and Osterman, G. B.: Characterization of OCO-2 and ACOS-GOSAT biases and errors for CO_2 flux estimates, (October), 2019.***

Page 30, lines 678–680: ***Velazco, V. A., Morino, I., Uchino, O., Hori, A., Kiel, M., Bukosa, B., Deutscher, N. M., Sakai, T., Nagai, T., Bagtasa, G., Izumi, T., Yoshida, Y. and Griffith, D. W. T.: TCCON Philippines: First measurement results, satellite data and model comparisons in Southeast Asia, Remote Sens., 9(12), 1–18, doi:10.3390/rs9121228, 2017.***

Comment

Page 8, line 210: Missing "N" in "20 –30 N" whilst in other instances you have used "20 N–30 N".

Response

The sentence is corrected as follows:

Page 9, lines 230–231: *At 20° **N**–30° N, the peak-to-trough amplitudes of the seasonal cycles at sea level is 8.5 ± 0.9 ppm, and is ~2 ppm larger than the amplitudes in the upper troposphere (6.5 ± 0.6 ppm).*

Comment

Figure A2: Add an x-label.

Response

The Figure A2 corresponds to Figure A3 of the revised manuscript. The x-label is revised as follows:

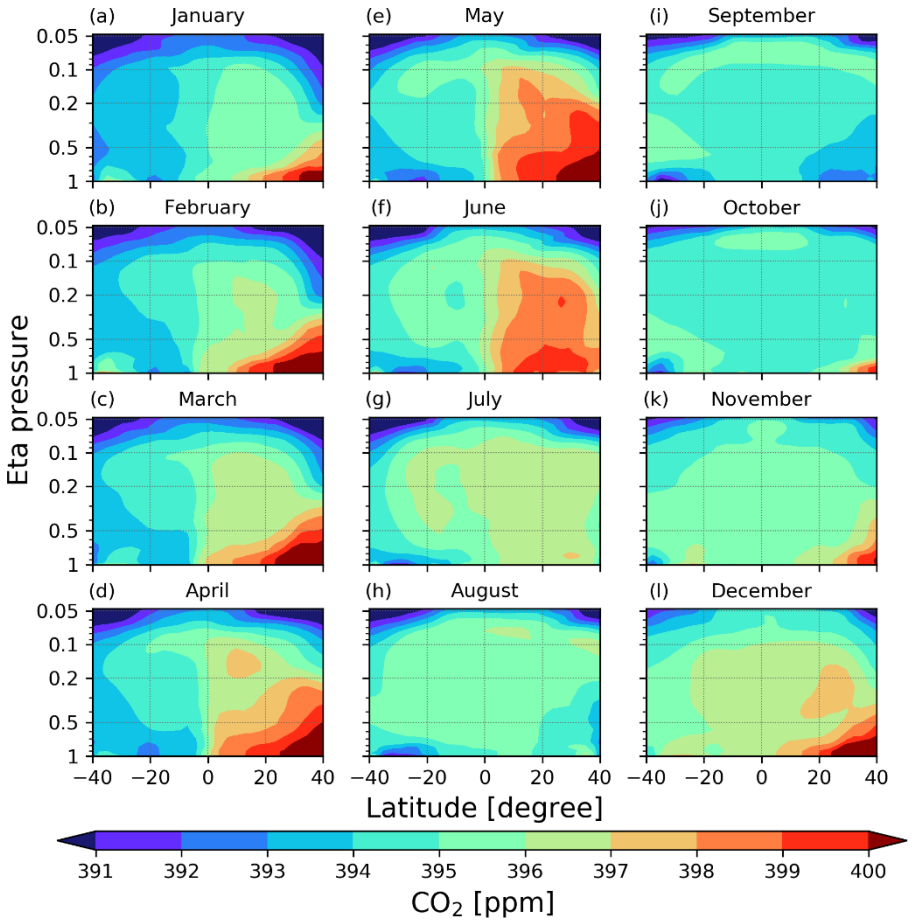

785 Page 23, lines 467–468: Figure A**3**. Latitude-pressure distribution of the inversion of the CO_2 mixing ratio at longitude 146° E in 2015, obtained from ACTM forward simulations.

Other corrections

We corrected a few values caused by a mistake in the calculation script, some typos, and inconsistent spellings as follows:

Page 2, lines 49–51: *The uneven distribution and limited spatial coverage of in situ measurements makes it **difficult** to infer CO_2 fluxes between the surface and the atmosphere on regional to global scales **at high accuracy** (Canadell et al., 2011; Chevallier et al., 2010, 2011).*

Pages 5–6, lines 151–160: *The details of the MIROC4-ACTM are described in Patra et al. (2018). In short, the MIROC4-ACTM uses a hybrid vertical coordinate to resolve gravity wave propagation in the stratosphere**, where at least 30 model layers reside**. The hybrid coordinate transitions from sigma coordinates at the surface to pressure levels around the tropopause. **In total, 67 vertical layers are used between the Earth's surface and 0.0128 hPa. The MIROC4-ACTM has a horizontal resolution of triangular 42 truncation (T42) which corresponds to approximately 2.8° longitude by 2.8° latitude.** The ACTMs are nudged with the Japanese 55-year Reanalysis (JRA-55; Kobayashi et al., 2015) for horizontal winds and temperature at Newtonian relaxation times of 1-hour and 5-hours, respectively. Nudging is performed for all the model layers from 2 to 60. A high accuracy of the MIROC4-ACTM is indicated by the agreement of simulated "age of air", which is a diagnostic for atmospheric transport, with that expected from measured sulphur hexafluoride (SF_6) and CO_2 in the troposphere and stratosphere, respectively (Patra et al., 2018). All data obtained over land are excluded **in the current study**.*

Page 9, lines 219–220: *The difference in XCO_2 was **only** 0.2 ± 0.1 ppm on average.*

Page 14, lines 324–325: *In all latitudes, **obs.** and satellite XCO_2 show an overall significant positive correlation (R^2: NIES = 0.84 ± 0.02, ACOS = 0.74 ± 0.0**8**, OCO-2 = 0.8**2** ± 0.0**5**) (Table 2).*

Page 14, lines 327–329: *The smallest **average** bias is found for NIES, likely due to the stricter quality filters as discussed in section 4.1. **While ACOS and OCO-2 show rather a systematic offset, the NIES retrieval seems to be more noisy (Figs. 5d and 5e, Table 3).***

Page 14, lines 329–330*: … and decreases by 40% (0.5**6** ppm) on average between the northernmost and southernmost regions (Table 2).*

Page 15, line 344:

	R^2			RMSE		
Latitude	*NIES*	*ACOS*	*OCO-2*	*NIES*	*ACOS*	*OCO-2*
20° N–30° N	*0.86*	*0.64*	*0.81*	*1.06*	*1.70*	*1.26*
0° N–10° N	*0.81*	*0.76*	*0.76*	*1.02*	*1.17*	*1.23*
20° S–10° S	*0.85*	*0.82*	*0.88*	*0.84*	*0.79*	*0.70*

Page 16, lines 346–348: *Table 3. Average (Avg.) difference and the standard deviation (SD.) between **obs.** and satellite XCO_2 from GOSAT (NIES, ACOS) and OCO-2 of each latitude range between 2014 and 2017.*

	*difference **obs**. XCO_2 – satellite XCO_2*					
Latitude	*Avg. NIES*	*SD.*	*Avg. ACOS*	*SD.*	*Avg. OCO-2*	*SD.*
20° N–30° N	*0.61*	*0.87*	*1.60*	*0.59*	*1.14*	*0.52*
0° N–10° N	*0.51*	*0.87*	*1.00*	*0.60*	*1.12*	*0.52*
20° S–10° S	*0.20*	*0.81*	*0.48*	*0.63*	*0.31*	*0.63*

Page 2, lines 63–64: *Since 2009, NASA's Atmospheric CO_2 Observation from Space (ACOS) and GOSAT team work closely together on the analysis of GOSAT observations (Crisp et al., 2012; O'Dell et al., 2012).*

Page 3, lines 79–81: *Comparisons of ACOS GOSAT XCO_2 estimates to those from HIAPER Pole-to-Pole Observations (HIPPO) campaigns (Frankenberg et al., 2016) show lower bias (−0.06 ppm) and standard deviation (0.45 ppm).*

Page 5, lines 136–137: *For ACOS and OCO-2, we chose data with a good quality flag (quality flag = 0), which is provided by each algorithm.*

Page 9, lines 226–228: *Average CO_2 mixing ratios of 402.9 ± 3.6 ppm and 401.2 ± 3.1 ppm at lower and upper troposphere, exceeded that from south of the equator by 4.5 ppm and 1.5 ppm, respectively.*

Pages 11–12, lines 277–278: *The coarse horizontal resolution of the model is not adequate to represent observations near source regions.*

Lines 196, 274, 279, 363: Changed from *MIROC-4 ACTM* to ***MIROC4-ACTM***

Lines 163, 224, 243: Changed *mid latitudes* to ***midlatitudes***

Lines 175, 228: 236, 273, 277, 280, 300: Changed *sea-level* to ***sea level***

Lines 295, 296, 297, 323, 327, 331, 413: Changed *Fig.* to ***Figs.***

References

Bisht, J. S. H., Machida, T., Chandra, N., Tsuboi, K., Patra, P. K., Umezawa, T., Niwa, Y., Sawa, Y., Morimoto, S., Nakazawa, T., Saitoh, N. and Takigawa, M.: Seasonal Variations of SF_6, CO_2, CH_4, and N_2O in the UT/LS Region due to Emissions, Transport, and Chemistry, J. Geophys. Res. Atmos., 126(4), 1–18, doi:10.1029/2020JD033541, 2021.

Canadell, J. G., Ciais, P., Gurney, K., Le Quéré, C., Piao, S., Raupach, M. R. and Sabine, C. L.: An International Effort to Quantify Regional Carbon Fluxes, Eos, Trans. Am. Geophys. Union, 92(10), 81–82, doi:10.1029/2011EO100001, 2011.

Chevallier, F., Ciais, P., Conway, T. J., Aalto, T., Anderson, B. E., Bousquet, P., Brunke, E. G., Ciattaglia, L., Esaki, Y., Fröhlich, M., Gomez, A., Gomez-Pelaez, A. J., Haszpra, L., Krummel, P. B., Langenfelds, R. L., Leuenberger, M., Machida, T., Maignan, F., Matsueda, H., Morguí, J. A., Mukai, H., Nakazawa, T., Peylin, P., Ramonet, M., Rivier, L., Sawa, Y., Schmidt, M., Steele, L. P., Vay, S. A., Vermeulen, A. T., Wofsy, S. and Worthy, D.: CO_2 surface fluxes at grid point scale estimated from a global 21 year reanalysis of atmospheric measurements, J. Geophys. Res., 115(D21), D21307, doi:10.1029/2010JD013887, 2010.

Chevallier, F., Deutscher, N. M., Conway, T. J., Ciais, P., Ciattaglia, L., Dohe, S., Fröhlich, M., Gomez-Pelaez, A. J., Griffith, D., Hase, F., Haszpra, L., Krummel, P., Kyrö, E., Labuschagne, C., Langenfelds, R., Machida, T., Maignan, F., Matsueda, H., Morino, I., Notholt, J., Ramonet, M., Sawa, Y., Schmidt, M., Sherlock, V., Steele, P., Strong, K., Sussmann, R., Wennberg, P., Wofsy, S., Worthy, D., Wunch, D. and Zimnoch, M.: Global CO_2 fluxes inferred from surface air-sample measurements and from TCCON retrievals of the CO_2 total column, Geophys. Res. Lett., 38(24), doi:10.1029/2011GL049899, 2011.

Connor, B. J., Boesch, H., Toon, G., Sen, B., Miller, C. and Crisp, D.: Orbiting Carbon Observatory: Inverse method and prospective error analysis, J. Geophys. Res. Atmos., 113(5), 1–14, doi:10.1029/2006JD008336, 2008.

Conway, T. J., Tans, P. P., Waterman, L. S., Thoning, K. W., Kitzis, D. R., Masarie, K. A. and Zhang, N.: Evidence for interannual variability of the carbon cycle from the National Oceanic and Atmospheric Administration/Climate Monitoring and Diagnostics Laboratory Global Air Sampling Network, J. Geophys. Res., 99(D11), 22831, doi:10.1029/94JD01951, 1994.

Crisp, D., Fisher, B. M., O'Dell, C., Frankenberg, C., Basilio, R., Bösch, H., Brown, L. R., Castano, R., Connor, B., Deutscher, N. M., Eldering, A., Griffith, D., Gunson, M., Kuze, A., Mandrake, L., McDuffie, J., Messerschmidt, J., Miller, C. E., Morino, I., Natraj, V., Notholt, J., O'Brien, D. M., Oyafuso, F., Polonsky, I., Robinson, J., Salawitch, R., Sherlock, V., Smyth, M., Suto, H., Taylor, T. E., Thompson, D. R., Wennberg, P. O., Wunch, D. and Yung, Y. L.: The ACOS CO_2 retrieval algorithm - Part II: Global XCO_2 data characterization, Atmos. Meas. Tech., 5(4), 687–707, doi:10.5194/amt-5-687-2012, 2012.

Crowell, S., Baker, D., Schuh, A., Basu, S., Jacobson, A. R., Chevallier, F., Liu, J., Deng, F., Feng, L., McKain, K., Chatterjee, A., Miller, J. B., Stephens, B. B., Eldering, A., Crisp, D., Schimel, D., Nassar, R., O'Dell, C. W., Oda, T., Sweeney, C., Palmer, P. I. and Jones, D. B. A.: The 2015–2016 carbon cycle as seen from OCO-2 and the global in situ network, Atmos. Chem. Phys., 19(15), 9797–9831, doi:10.5194/acp-19-9797-2019, 2019.

Dlugokencky, E. and Tans, P.: Trends in Atmospheric Carbon Dioxide. NOAA/GML; www.esrl.noaa.gov/gmd/ccgg/trends/, last access: 7 January 2021.

Frankenberg, C., Kulawik, S. S., Wofsy, S. C., Chevallier, F., Daube, B., Kort, E. A., O'Dell, C., Olsen, E. T. and Osterman, G.: Using airborne HIAPER pole-to-pole observations (HIPPO) to evaluate model and remote sensing estimates of atmospheric carbon dioxide, Atmos. Chem. Phys., 16(12), 7867–7878, doi:10.5194/acp-16-7867-2016, 2016.

Hakkarainen, J., Ialongo, I., Maksyutov, S. and Crisp, D.: Analysis of Four Years of Global XCO_2 Anomalies as Seen by Orbiting Carbon Observatory-2, Remote Sens., 11(7), 850, doi:10.3390/rs11070850, 2019.

Inai, Y., Aoki, S., Honda, H., Furutani, H., Matsumi, Y., Ouchi, M., Sugawara, S., Hasebe, F., Uematsu, M. and Fujiwara, M.: Balloon-borne tropospheric CO_2 observations over the equatorial eastern and western Pacific, Atmos. Environ., 184(December 2017), 24–36, doi:10.1016/j.atmosenv.2018.04.016, 2018.

Inoue, M., Morino, I., Uchino, O., Miyamoto, Y., Yoshida, Y., Yokota, T., Machida, T., Sawa, Y., Matsueda, H., Sweeney, C., Tans, P. P., Andrews, A. E., Biraud, S. C., Tanaka, T., Kawakami, S. and Patra, P. K.: Validation of XCO_2 derived from SWIR spectra of GOSAT TANSO-FTS with aircraft measurement data, Atmos. Chem. Phys, 13, 9771–9788, doi:10.5194/acp-13-9771-2013, 2013.

Kobayashi, S., Ota, Y., Harada, Y., Ebita, A., Moriya, M., Onoda, H., Onogi, K., Kamahori, H., Kobayashi, C., Endo, H., Miyaoka, K. and Takahashi, K.: The JRA-55 Reanalysis: General Specifications and Basic Characteristics, J. Meteorol. Soc. Japan. Ser. II, 93(1), 5–48, doi:10.2151/jmsj.2015-001, 2015.

Kulawik, S. S., Crowell, S., Baker, D., Liu, J., Mckain, K., Sweeney, C., Biraud, S. C., Wofsy, S., Dell, C. W. O., Wennberg, P. O., Wunch, D., Roehl, M., Deutscher, N. M., Kiel, M., Griffith, D. W. T., Velazco, V. A., Dubey, M. K., Sepulveda, E., Elena, O., Rodriguez, G., Té, Y., Heikkinen, P., Dlugokencky, E. J., Gunson, M. R., Eldering, A., Fisher, B. and Osterman, G. B.: Characterization of OCO-2 and ACOS-GOSAT biases and errors for CO_2 flux estimates, , (October), 2019.

Laughner, J., Andrews, A., Roche, S., Kiel, M. and Toon, G.: ginput v1.0.7b: GGG2020 prior profile software, CaltechDATA., 2021.

Laughner, J.L.; Kiel, M.; Toon, G.; Andrews, A.; Roche, S.; Wunch, D.; Wennberg, P.O. (in prep). Revised formulation of the TCCON priors for GGG2020.

Matsueda, H., Machida, T., Sawa, Y., Nakagawa, Y., Hirotani, K., Ikeda, H., Kondo, N. and Goto, K.: Evaluation of atmospheric CO_2 measurements from new flask air sampling of JAL airliner observations, Pap. Meteorol. Geophys., 59(March), 1–17, doi:10.2467/mripapers.59.1, 2008.

Morino, I., Tsutsumi, Y., Uchino, O., Ohyama, H., Thi Ngoc Trieu, T., Frey, M. M., Yoshida, Y., Matsunaga, T., Kamei, A., Saito, M. and Noda, H. M.: Status of GOSAT and GOSAT-2 FTS SWIR L2 Product Validation, in The 16th International Workshop on Greenhouse Gas Measurement from Space, pp. 2–5., 2020.

Niwa, Y., Patra, P. K., Sawa, Y., MacHida, T., Matsueda, H., Belikov, D., Maki, T., Ikegami, M., Imasu, R., Maksyutov, S., Oda, T., Satoh, M. and Takigawa, M.: Three-dimensional variations of atmospheric CO_2: Aircraft measurements and multi-transport model simulations, Atmos. Chem. Phys., 11(24), 13359–13375, doi:10.5194/acp-11-13359-2011, 2011.

O'Dell, C. W., Connor, B., Bösch, H., O'Brien, D., Frankenberg, C., Castano, R., Christi, M., Eldering, D., Fisher, B., Gunson, M., McDuffie, J., Miller, C. E., Natraj, V., Oyafuso, F., Polonsky, I., Smyth, M., Taylor, T., Toon, G. C., Wennberg, P. O. and Wunch, D.: The ACOS CO_2 retrieval algorithm-Part 1: Description and validation against synthetic observations, Atmos. Meas. Tech., 5(1), 99–121, doi:10.5194/amt-5-99-2012, 2012.

O'Dell, C. W., Eldering, A., Wennberg, P. O., Crisp, D., Gunson, M. R., Fisher, B., Frankenberg, C., Kiel, M., Lindqvist, H., Mandrake, L., Merrelli, A., Natraj, V., Nelson, R. R., Osterman, G. B., Payne, V. H., Taylor, T. E., Wunch, D., Drouin, B. J., Oyafuso, F., Chang, A., McDuffie, J., Smyth, M., Baker, D. F., Basu, S., Chevallier, F., Crowell, S. M. R., Feng, L., Palmer, D. P. I., Dubey, M., García, O. E., Griffith, D. W. T., Hase, F., Iraci, L. T., Kivi, R., Morino, I., Notholt, J., Ohyama, H., Petri, C., Roehl, C. M., Sha, M. K., Strong, K., Sussmann, R., Te, Y., Uchino, O. and Velazco, V. A.: Improved retrievals of carbon dioxide from Orbiting Carbon Observatory-2 with the version 8 ACOS algorithm, Atmos. Meas. Tech., 11(12), 6539–6576, doi:10.5194/amt-11-6539-2018, 2018.

Ohyama, H., Morino, I., Velazco, V. A., Klausner, T., Bagtasa, G., Kiel, M., Frey, M., Hori, A., Uchino, O., Matsunaga, T., Deutscher, N. M., DiGangi, J. P., Choi, Y., Diskin, G. S., Pusede, S. E., Fiehn, A., Roiger, A., Lichtenstern, M., Schlager, H., Wang, P. K., Chou, C. C.-K., Andrés-Hernández, M. D. and Burrows, J. P.: Validation of XCO_2 and XCH_4 retrieved from a portable Fourier transform spectrometer with those from in situ profiles from aircraft-borne instruments, Atmos. Meas. Tech., 13(10), 5149–5163, doi:10.5194/amt-13-5149-2020, 2020.

Patra, P. K., Maksyutov, S., Sasano, Y., Nakajima, H., Inoue, G. and Nakazawa, T.: An evaluation of CO_2 observations with Solar Occultation FTS for Inclined-Orbit Satellite sensor for surface source inversion, J. Geophys. Res. Atmos., 108(D24), doi:10.1029/2003JD003661, 2003.

Patra, P. K., Takigawa, M., Watanabe, S., Chandra, N., Ishijima, K. and Yamashita, Y.: Improved chemical tracer simulation by MIROC4.0-based atmospheric chemistry-transport model (MIROC4-ACTM), Sci. Online Lett. Atmos., 14, 91–96, doi:10.2151/SOLA.2018-016, 2018.

Umezawa, T., Matsueda, H., Sawa, Y., Niwa, Y., Machida, T. and Zhou, L.: Seasonal evaluation of tropospheric CO_2 over the Asia-Pacific region observed by the CONTRAIL commercial airliner measurements, Atmos. Chem. Phys., 18(20), 14851–14866, doi:10.5194/acp-18-14851-2018, 2018.

Velazco, V. A., Morino, I., Uchino, O., Hori, A., Kiel, M., Bukosa, B., Deutscher, N. M., Sakai, T., Nagai, T., Bagtasa, G., Izumi, T., Yoshida, Y. and Griffith, D. W. T.: TCCON Philippines: First measurement results, satellite data and model comparisons in Southeast Asia, Remote Sens., 9(12), 1–18, doi:10.3390/rs9121228, 2017.

Wofsy, S. C.: HIAPER Pole-to-Pole Observations (HIPPO): fine-grained, global-scale measurements of climatically important atmospheric gases and aerosols, Philos. Trans. R. Soc. A Math. Phys. Eng. Sci., 369(1943), 2073–2086, doi:10.1098/rsta.2010.0313, 2011.

Wofsy, S. C., Afshar, S., Allen, H. M., Apel, E., Asher, E. C., Barletta, B., Bent, J., Bian, H., Biggs, B. C., Blake, D. R., Blake, N., Bourgois, I., Brock, C. A., Brune, W. H., Budney, J. W., Bui, T. P., Butler, A., Campuzano-Jost, P., Chang, C. S., Chin, M., Commane, R., Correa, G., Crounse, J. D., Cullis, P. D., Daube, B. C., Day, D. A., Dean-Day, J. M., Dibb, J. E., Digangi, J. P., Diskin, G. S., Dollner, M., Elkins, J. W., Erdesz, F., Fiore, A. M., Flynn, C. M., Froyd, K., Gesler, D. W., Hall, S. R., Hanisco, T. F., Hannun, R. A., Hills, A. J., Hintsa, E. J., Hoffmann, A., Hornbrook, R. S., Huey, L. G., Hughes, S., Jimenez, J. L., Johnson, B. J., Katich, J. M., Keeling, R., Kim, M. J., Kupc, A., Lait, L. R., Lamarque, J.-F., Liu, H. B., McKain, K., Mclaughlin, R. J., Meinardi, S., Miller, D. O., Montzka, S. A., Moore, F. L., Morgan, E. J., Murphy, D. M., Murray, L. T., Nault, B. A., Neuman, J. A., Newman, P. A., Nicely, J. M., Pan, X., Paplawsky, W., Peischl, J., Prather, M. J., Price, D. J., Ray, E., Reeves, J. M., Richardson, M., Rollins, A. W., Rosenlof, K. H., Ryerson, T. B., Scheuer, E., Schill, G. P., Schroder, J. C., Schwarz, J. P., St.Clair, J. M., Steenrod, S. D., Stephens, B. B., Strode, S. A., Sweeney, C., Tanner, D., Teng, A. P., Thames, A. B., Thompson, C. R., Ullmann, K., Veres, P. R., Vizenor, N., Wagner, N. L., Watt, A., Weber, R., Weinzierl, B., et al.: ATom: Merged Atmospheric Chemistry, Trace Gases, and Aerosols, , doi:10.3334/ORNLDAAC/1581, 2018.

Wunch, D., Toon, G. C., Blavier, J.-F. L., Washenfelder, R. A., Notholt, J., Connor, B. J., Griffith, D. W. T., Sherlock, V. and Wennberg, P. O.: The Total Carbon Column Observing Network, Philos. Trans. R. Soc. A Math. Phys. Eng. Sci., 369(1943), 2087–2112, doi:10.1098/rsta.2010.0240, 2011.

Yoshida, Y., Ota, Y., Eguchi, N., Kikuchi, N., Nobuta, K., Tran, H., Morino, I. and Yokota, T.: Retrieval algorithm for CO_2 and CH_4 column abundances from short-wavelength infrared spectral observations by the Greenhouse gases observing satellite, Atmos. Meas. Tech., 4(4), 717–734, doi:10.5194/amt-4-717-2011, 2011.

Yoshida, Y., Kikuchi, N., Morino, I., Uchino, O., Oshchepkov, S., Bril, A., Saeki, T., Schutgens, N., Toon, G. C., Wunch, D., Roehl, C. M., Wennberg, P. O., Griffith, D. W. T., Deutscher, N. M., Warneke, T., Notholt, J., Robinson, J., Sherlock, V., Connor, B., Rettinger, M., Sussmann, R., Ahonen, P., Heikkinen, P., Kyrö, E., Mendonca, J., Strong, K., Hase, F., Dohe, S. and Yokota, T.: Improvement of the retrieval algorithm for GOSAT SWIR XCO_2 and XCH_4 and their validation using TCCON data, Atmos. Meas. Tech., 6(6), 1533–1547, doi:10.5194/amt-6-1533-2013, 2013.

New approach to evaluate satellite derived XCO_2 over oceans by integrating ship and aircraft observations

Astrid Müller[1], Hiroshi Tanimoto[1], Takafumi Sugita[1], Toshinobu Machida[1], Shin-ichiro Nakaoka[1], Prabir K. Patra[2], Joshua Laughner[3], David Crisp[4]

1 National Institute for Environmental Studies, Tsukuba, Japan
2 Japan Agency for Marine-Earth Science and Technology, Yokohama, Japan
3 California Institute of Technology, Pasadena, CA, USA
4 Jet Propulsion Laboratory/California Institute of Technology, Pasadena, CA, USA

Correspondence and request for material should be addressed to:
Hiroshi Tanimoto (tanimoto@nies.go.jp), Astrid Müller (mueller.astrid@nies.go.jp)

Abstract. Satellite observations provide spatially-resolved global estimates of column-averaged mixing ratios of CO_2 (XCO_2) over the Earth's surface. The accuracy of these datasets can be validated against reliable standards in some areas, but other areas remain inaccessible. To date, limited reference data over oceans hinders successful uncertainty quantification or bias correction efforts, and precludes reliable conclusions about changes in the carbon cycle in some regions. Here, we propose a new approach to analyze and evaluate seasonal, interannual and latitudinal variations of XCO_2 over oceans by integrating cargo-ship (SOOP, Ship Of Opportunity) and commercial aircraft (CONTRAIL, Comprehensive Observation Network for Trace gases by Airliner) observations with the aid of state-of-the art atmospheric chemistry-transport model calculations. The consistency of the "observation-~~in situ~~ based column-averaged CO_2" dataset (obs.~~in situ~~ XCO_2) with satellite estimates was analyzed over the Western Pacific between 2014 and 2017, and its utility as reference dataset evaluated. Our results demonstrate that the new dataset accurately captures seasonal and interannual variations of CO_2. Retrievals of XCO_2 over the ocean from GOSAT (Greenhouse gases observing satellite: NIES v02.75, National Institute for Environmental Studies; ACOS v7.3, Atmospheric CO_2 Observation from Space) and OCO-2 (Orbiting Carbon Observatory, v9r) observations show a negative bias of about 1 parts per million (ppm) in northern midlatitudes, which was attributed to measurement uncertainties of the satellite observations. The NIES retrieval had higher consistency with obs.~~in situ~~ XCO_2 at midlatitudes as compared to the other retrievals. At low latitudes, it shows many fewer valid data and high scatter, such that ACOS and OCO-2 appear to provide a better representation of the carbon cycle. At different times, the seasonal cycles of all three retrievals show positive phase shifts of one month relative to the observation-based~~in situ~~ data. The study indicates that even if the retrievals complement each other, remaining uncertainties limit the accurate interpretation of spatiotemporal changes in CO_2 fluxes. A continuous long-term XCO_2 dataset with wide latitudinal coverage based on the new approach has a great potential as a robust

reference dataset for XCO_2 and can help to better understand changes in the carbon cycle in response to climate change using satellite observations.

1 Introduction

Efforts to control the accelerated increase of carbon dioxide (CO_2) in the atmosphere became a serious international task in the last decades. CO_2 is the most important anthropogenic greenhouse gas (GHG). Since the beginning of the Industrial Era in the 1750s, fossil fuel combustion and other human activities have increased the atmospheric concentration of CO_2 from approximately 277 ppm to more than 4107 ppm in 201820 (Friedlingstein et al., 2019) (Dlugokencky, E. and Tans P.: Trends in Atmospheric Carbon Dioxide, NOAA/GML; www.esrl.noaa.gov/gmd/ccgg/trends/, last access: 7 January 2021). On average, less than half of the anthropogenic CO_2 emitted each year stays in the atmosphere, as the ocean and land each capture approximately one-fourth (Friedlingstein et al., 2019). Seasonal changes in CO_2 uptake and release alter the fraction of atmospheric CO_2 substantially and lead to year-to-year variations, which are not yet fully understood (e.g. Friedlingstein et al., 2019; Intergovernmental Panel on Climate Change (IPCC), 2013). As the carbon cycle responds to a changing climate, a comprehensive understanding of changes in CO_2 sources and sinks is crucial to the implementation of effective strategies for reducing global warming.

In situ measurements from ground-based networks and aircraft campaigns provide precise information on local CO_2 concentrations. There are now more than 100 surface measurement sites around the globe, but most are located on land in nNorth America and Europe, and some in the East Asia and Oceania, and few in other continents (e.g., Crowell et al., 2019; Hakkarainen et al., 2019). Very few sites are located over the open oceans, even though 70% of the Earth's surface is covered by water and the ocean is a key element of the global carbon cycle. The uneven distribution and limited spatial coverage of in situ measurements makes it impossible difficult to infer CO_2 fluxes between the surface and the atmosphere on regional to global scales at high accuracy (Canadell et al., 2011; Chevallier et al., 2010, 2011). Space-based remote sensing measurements are complementing in situ observations. Their high spatial and temporal coverage allows observation of changes in atmospheric CO_2 mixing ratios even in regions with poor in situ coverage (Baker et al., 2010, Crisp et al., 2012). By collecting high resolution spectra of near infrared (NIR) and shortwave infrared (SWIR) solar radiation reflected from the Earth's surface, satellite observations can yield estimates of the total atmospheric column of CO_2. These observations are most sensitive to the lower troposphere where CO_2 is most variable (Patra et al., 2003) and therefore, are able to improves the knowledge on local CO_2 emission and sinks (Connor et al., 2008).

Japan's Greenhouse gases Observing Satellite (GOSAT), and the second NASA's (National Aeronautics and Space Administration) Orbiting Carbon Observatory (OCO-2) are dedicated to inferring the concentration of GHGs from high-resolution spectra at NIR and SWIR wavelengths. Since their launches in 2009 and 2014, GOSAT and OCO-2 have successfully provided global datasets of column-averaged mixing ratios of CO_2 (XCO_2). In 2018, GOSAT-2 was launched,

aiming to improve the measurement precision and to overcome anomalies of the spectrometer on board GOSAT (Nakajima et al., 2017). The launch of OCO-3 followed in 2019. Since 2009, NASA's Atmospheric CO_2 Observation from Space (ACOS) and GOSAT team work closely together on the analysis of GOSAT observations (Crisp et al., 2012; O'Dell et al., 2012). Comparisons of XCO_2 generated by the GOSAT team of the National Institute for Environmental Studies (NIES) (e.g., Yoshida et al., 2013) with that of the ACOS retrieval algorithm are aimed to improve the accuracy of the estimated XCO_2.

Variations in the CO_2 concentration associated with surface sources and sinks are typically not larger than 1 ppm (0.25%), and annual and seasonal variations of XCO_2 are small compared to the mean abundance in the atmosphere (Crisp et al., 2012; Miller et al., 2007). Therefore, a precision of 1–2 ppm for CO_2 satellite retrievals is needed (Crisp et al., 2012). Any uncharacterized systematic errors in the retrieval affect the accuracy of XCO_2 and limit its utility for carbon cycle studies (Basu et al., 2013). Therefore, extensive validation of satellite XCO_2 has been performed, mainly against data of the Total Carbon Column Observing Network (TCCON) (Wunch et al., 2011), which is a network of ground-based Fourier transform infrared (FTIR) spectrometers. However, TCCON sites are land based and~~has a~~ very limited number of sites observe the atmosphere over~~ing~~ open oceans, which are defined as the ocean area outside the coastal region. Between the GOSAT NIES soundings over the ocean~~retrieval~~ and TCCON sites near the ocean, a bias of -1.09 ± 2.27 ppm was found (Morino et al., 2020). Negative XCO_2 anomalies north and south of the equator are observed in the OCO-2 retrieval over the Pacific Ocean (Hakkarainen et al., 2019). In combination with surface measurements, vertical profiles of CO_2 obtained by aircraft~~s~~ can constrain XCO_2 but are very limited (e.g., Frankenberg et al., 2016; Inoue et al., 2013; Wofsy, 2011; Wofsy et al., 2018). Inoue et al. (2013) found a bias as large as −1.8 to −2.3 ppm between aircraft-based XCO_2 and that from GOSAT NIES at the Pacific Ocean. Comparisons of ACOS GOSAT XCO_2 estimates to those from HIAPER Pole-to-Pole Observations (HIPPO) campaigns (Frankenberg et al., 2016) show lower bias (−0.06 ppm) and ~~a~~ standard deviation (0.45 ppm). More recent comparisons of OCO-2 XCO_2 estimates to in situ measurements from the NASA Atmospheric Tomography Mission reveals a systematic bias of ~~−~~−0.7 ppm over the tropical Pacific, that is also seen in ~~TCCON~~ the data at Burgos, a TCCON station in that region (Kulawik et al., 2019; Velazco et al., 2017~~, Atmos. Meas. Tech. Discuss., https://doi.org/10.5194/amt-2019-257~~). Limited reference data in the tropical and high latitudinal oceans are the reason for major uncertainties in satellite retrievals over these regions. Therefore, variations in XCO_2 over ocean sites cannot be reliably captured, but this is necessary for modeling the future climate (e.g., Crowell et al., 2019).

We propose a new approach to analyze and evaluate seasonal, interannual and latitudinal variations of satellite derived XCO_2 by integrating cargo-ship and commercial aircraft observations. We use long-term datasets of the dry air mole fraction of CO_2 from Japan's CONTRAIL (Comprehensive Observation Network for Trace gases by Airliner) and SOOP (Ship Of Opportunity) project which cover wide latitudinal and longitudinal regions of the Pacific and South China Sea. Together with state-of-the art atmospheric chemistry-transport model calculations (Patra et al., 2018), we calculate observation-~~in situ~~ based XCO_2. The consistency of the spatiotemporal variation of the ship-aircraft based XCO_2 with satellite estimates from OCO-2, and two GOSAT retrievals (NIES, ACOS) is analyzed, and its utility as long-term reference dataset evaluated.

2 Observational Data

2.1 Aircraft

Japan's Comprehensive Observation Network for Trace gases by Airliner, CONTRAIL, uses commercial aircraft flying between Japan and Europe, Asia, Australia, Hawaii and North America to continuously measure atmospheric CO_2 since 2005. In cooperation with Japan Airlines (JAL), the Continuous CO_2 Measuring Equipment (CME) is installed in the forward cargo compartment on 777-200ER or 777-300ER aircraft (Machida et al., 2008; Umezawa et al., 2018). The CME measures the CO_2 dry mole fraction using a non-dispersive infrared gas analyzer (NDIR; LI-840, LI-COR Biogeosciences). Air samples are taken from the air conditioning system of the aircraft. Before the samples are analyzed by the NDIR, a diaphragm pump draws the samples through a drier tube packed with CO_2-saturated magnesium perchlorate to remove water vapor. The flow rate and absolute pressure in the NDIR are kept constant by a mass flow controller and auto pressure controller, respectively.

Two standard gases are introduced into the NDIR every 14 minutes (min) during the ascent and decent portions of the flight and every 62 min during the cruise at 8-12 km height (Machida et al., 2008; Umezawa et al., 2018). Forty seconds (s) after the switch from standard gas to air sample, data are collected as averages of 10 s during the ascent and decent, and 1 min averages during the cruise (~ 15 km horizontal distance). Data of each 10 s and 1 min period are rejected if the standard deviation ~~does not~~ exceeds 3 ppm (Umezawa et al., 2018). The analytical uncertainty of the CME is 0.2 ppm, which was estimated from the comparison with occasional flask sampling, using an automatic air sampling equipment (Matsueda et al., 2008).

In this study, we used CME data v2019.1.0 from flights between Narita and Sydney over the Western Pacific Ocean between 2014 and 2017. Only those data which were obtained below the tropopause height during the cruise at around 11 km altitude are used. To define the tropopause height, we used the blended tropopause pressure (TROPPB), which is explained in detail in **section 3.2**. Data of the lower stratosphere were only occasionally obtained. We screened out those data in order to have a consistent methodology for constructing CO_2 profiles as explained in **section 3.2**.

2.2 Ship

Commercial cargo Ships of Opportunity (SOOP) have been collecting samples of atmospheric CO_2 on cruises since 2001 between Japan and North America, since 2005 between Japan and Australia and New Zealand, and since 2007, between Japan and South East Asia. In this study, we used data collected by the cargo ship Trans Future 5 (Toyofuji Shipping Co., Ltd.), which sails between Japan, Australia, and New Zealand. The dry air mole fraction of CO_2 is measured by a NDIR (MOG-701, Kimoto Electric Co.) every 10 s with an accuracy of 0.1 ppm. The NDIR is installed on top of the bridge at approximately 30 m above sea level (Yamagishi et al., 2012). Samples are drawn into the NDIR through a tube, whose inlet is placed at a location which is not affected by smoke of the ship. Calibration is done every 6 hours by introducing four CO_2 standards (360, 380, 400, 420 ppm, Taiyo Nippon Sanso Corporation, Japan).

2.3 Satellite

Japan's GOSAT launched in 2009, and NASA's OCO-2 launched in 2014, were developed to characterize the variability of the atmospheric CO_2 fraction at regional scales over the globe. Both the OCO-2 grating spectrometer and the Thermal And Near infrared Sensor for carbon Observations – Fourier Transform Spectrometer (TANSO-FTS) instrument on board GOSAT measure the reflected sunlight in three shortwave infrared (SWIR) channels: at around 0.764 µm, which contains significant O_2 absorption, at 1.61 µm which contains a weak CO_2 absorption band, and at 2.06 µm, containing a strong CO_2 absorption band (Crisp et al., 2017; Kuze et al., 2009). By measuring the amount of light absorbed by CO_2 and O_2, the column average CO_2 dry air mole fraction (XCO_2) is estimated by taking ratio of the total column amounts of CO_2 and ~~O_2, where O_2 provides an estimate for~~ the total column of dry air (O'Dell et al., 2012, 2018; Wunch et al., 2011; Yoshida et al., 2011, 2013).

When the launch system failed for the first OCO in 2009, the ACOS team modified the retrieval algorithm originally developed for OCO to allow GOSAT retrievals (O'Dell et al., 2012). In this study, we selected level 2 XCO_2 data in sun-glint mode from the NIES v02.75 (Yoshida et al., 2013), ACOS v7.3, and OCO-2 v9r retrieval algorithm, all of which were bias corrected. NIES v02.75 uses only cloud-free scenes. For ACOS and OCO-2, we chose data with a good quality flag (quality~~_~~ flag = 0), which is provided by each algorithm. The ACOS data processing is ongoing and data of version 7.3 are available until June 2016. At the time of writing the manuscript, ACOS version 9 was released. This version is based on a newer version of the GOSAT Level 1 product, which includes extended sun-glint data. Furthermore, OCO-2 version 10 was released. An initial comparison between ACOS v7.3 and v9~~r~~, and between OCO-2 v9r and v10 is included in the ~~supplement~~ Appendix A (Figs. A1 and A2) and section 5 Conclusions. In the following, we refer to data obtained by OCO-2 v9r and GOSAT using the retrieval algorithm from NIES v02.75 and ACOS v7.3 simply as "OCO-2", "NIES", and "ACOS", respectively.

3 Methodology

3.1 Data selection

In order to compare data of all satellite retrievals, we chose the time period from 2014 to 2017, when both GOSAT (NIES, ACOS) and OCO-2 XCO_2 products are available. Over the Western Pacific between 40° N and 30° S, we made 10° latitude by 20° longitude wide boxes around the ship and aircraft data in order to obtain enough co-located data for the seasonal and interannual comparison with satellite retrievals **(Fig. 1)**. Within these boxes, no significant latitudinal and longitudinal variation of the CO_2 mixing ratio is expected (Sawa et al., 2012). Results of the MIROC~~-~~4 (Model for Interdisciplinary Research On Climate Earth System, version 4.0)-based Atmospheric Chemistry Transport model (ACTM) were obtained for each hourly averaged location of the aircraft ~~(details are explained below)~~. The details of the MIROC4-ACTM are described in Patra et al. (2018). In short, the MIROC4-ACTM uses a hybrid vertical coordinate to resolve gravity wave propagation in the stratosphere, where at least 30 model layers reside. The hybrid coordinate transitions from sigma coordinates at the surface to pressure levels around the tropopause. In total, 67 vertical layers are used between the Earth's surface and 0.0128 hPa. The MIROC4-ACTM

has a horizontal resolution of triangular 42 truncation (T42) which corresponds to approximately 2.8° longitude by 2.8° latitude. The ACTMs are nudged with the Japanese 55-year Reanalysis (JRA-55; Kobayashi et al., 2015) for horizontal winds and temperature at Newtonian relaxation times of 1-hour and 5-hours, respectively. Nudging is performed for all the model layers from 2 to 60. A high accuracy of the MIROC4-ACTM is indicated by the agreement of simulated "age of air", which is a diagnostic for atmospheric transport, with that expected from measured sulphur hexafluoride (SF_6) and CO_2 in the troposphere and stratosphere, respectively (Patra et al., 2018). All data obtained over land are excluded in the current study. For the analysis of the seasonal and interannual variation of CO_2, we chose the ~~The~~ monthly averages of the satellite, in situ, and model datasets ~~are used for the further analysis~~. In this study, we focus on the results of the latitude ranges 20° N–30° N, 0° N–10° N, and 20° S–10° S, as representative for the northern mid-latitude, the equator region, and southern latitudes, respectively.

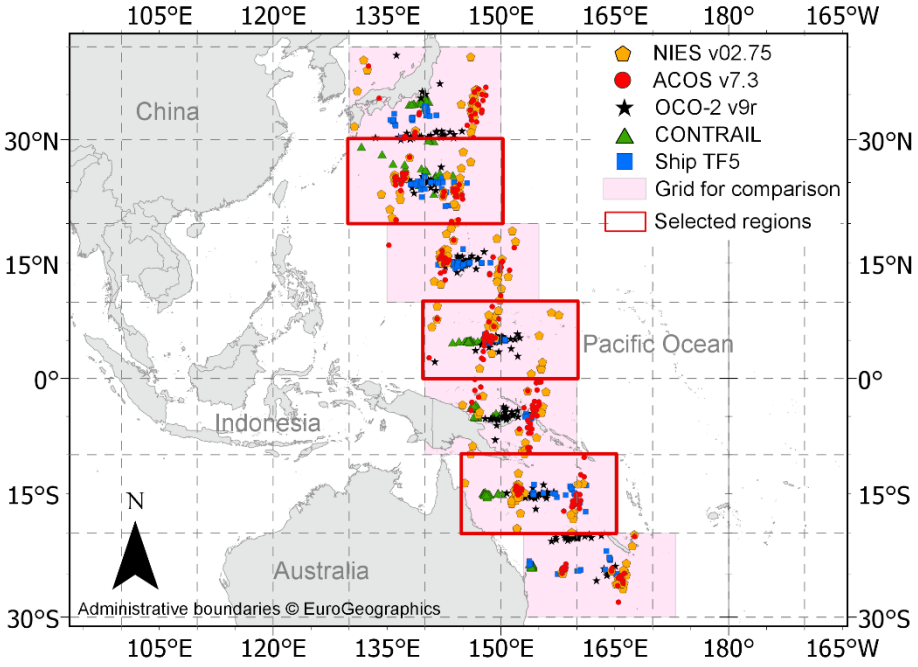

Figure 1. Location of monthly averaged data of CO_2 from aircraft (CONTRAIL, green triangle), ship (Trans Future 5 - TF5, blue squares), the satellite retrievals from NIES (yellow diamonds), ACOS (red circles), and OCO-2 (black stars) between 2014 and 2017. Selected regions within 10° latitude by 20° longitude boxes are shown in red frames. Administrative boundaries © EuroGeographics.

3.2 ~~In situ~~Observation-based CO_2 profile construction and XCO_2 calculation

Figure 2 shows how atmospheric CO_2 profiles are constructed with the aid of ship and aircraft data in order to derive column averaged mixing ratios of CO_2. Ship data are extrapolated vertically to ~850 hPa, which corresponds to the 3rd and 4th pressure

level of NIES and ACOS, respectively, counted from the surface. We chose this cut off as it represents the boundary layer above sea level in which most of the rapid variation of CO_2 occur. Previous balloon and aircraft measurements by the HIPPO campaign over the Tropical Eastern and Western Pacific showed stronger CO_2 variation of about 1 to 2 ppm within the first 2 km above sea -level. Above this level, the CO_2 mixing ratios were rather stable or kept changing linearly up to about the tropopause height (Frankenberg et al., 2016; Inai et al., 2018). To account for that variation within the boundary layer, we added a ±2 ppm uncertainty to the CO_2 estimates at ~850 hPa~~of that pressure level~~. Aircraft data from the cruise portion of the flight, which is usually between 380 and 200 hPa, are selected. These aircraft data are extrapolated down to the lower cruising height limit at 380 hPa, and at 30° N–40° N at 400 hPa. Furthermore, the aircraft data is also extrapolated upwards to the ~~The~~ blended tropopause pressure (TROPPB) ~~is used as upper limit for the extrapolation~~.

The TROPPB~~It~~ is defined as a combination of a thermal tropopause- and dynamic tropopause pressure (Wilcox et al., 2012). The TROPPB data are extracted from GEOS-FP (Goddard Earth Observing System – forward processing) meteorology data using the python suite "ginput" version 1.0.6 (Laughner et al., 2021). Ginput was developed to generate a priori vertical mixing ratios of chemical species (e.g., CO_2, CO, CH_4, N_2O) for the open source TCCON retrieval algorithm, GGG2020 (Laughner et al., in prep). The TROPPB was calculated every 3 hours on the 5th, 15th, and 25th of each month for each centre location of the 10° latitude by 20° longitude boxes. Between 2014 and 2017, the highest monthly variation was found at 20° N–30° N with a standard deviation ranging from 0 to 24 hPa (0.02 to 23.77 hPa) and an average standard deviation of 10 ± 5 hPa. The maximum difference of 24 hPa at the level of the TROPPB corresponds to difference in the altitude of 1 to 2 km. Assuming a straight profile between the extrapolated aircraft and ship data, we linearly interpolate in both pressure and volume mixing ratio.

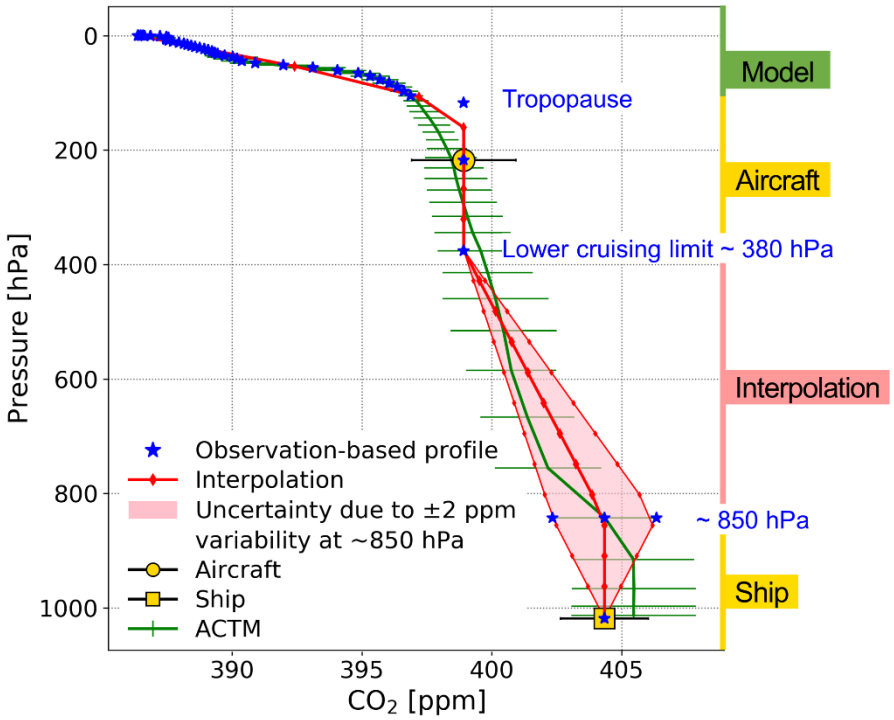

Figure 2. Construction of the ~~in situ adjusted~~ observation-based CO_2 profile (blue) obtained by using ship (SOOP) and aircraft (CONTRAIL) data (yellow) together with the results of the ACTM (green), and the interpolation (red). The example is obtained at the latitude 20° N–30° N, March 2014.

Total column observations in the atmosphere consists of up to 40% air in the stratosphere (Patra et al., 2018). To account for the stratospheric partial column, we used results of the MIROC-4--ACTM (Patra et al., 2018) above the TROPPB (**Fig. 2**) instead of the results from ginput. First, by using the MIROC4-ACTM, our method is fully independent of TCCON, which is important for using our methodology as a complement to TCCON to evaluate satellite retrievals. Second, the MIROC4-ACTM uses realistic flux and transport simulations and is one of the best validated stratospheric models at present. ~~The details of the MIROC-4 ACTM are described in Patra et al. (2018). In short, the MIROC-4 ACTM uses a hybrid vertical coordinate to resolve gravity wave propagation into the stratosphere. The hybrid coordinate transitions from sigma coordinates at the surface to pressure levels around the tropopause. The ACTMs are nudged with the Japanese 55-year Reanalysis (JRA-55; Kobayashi et al., 2015) for horizontal winds and temperature at Newtonian relaxation times of 1 hour and 5 hours, respectively. Nudging is performed for all the model layers from 2 to 60. In total, 67 vertical layers are used between the Earth's surface and 0.0128 hPa. A high accuracy of the MIROC-4 ACTM is indicated by the agreement of simulated "age of air", which is a diagnostic for atmospheric transport, with that expected from measured sulphur hexafluoride (SF_6) and CO_2 in the troposphere and stratosphere, respectively (Patra et al., 2018).~~

To calculate the XCO_2 that the satellite would have seen given the CO_2 profile constructed from in situ data, we first interpolate these profiles onto the corresponding monthly averaged pressure grid of the ACOS and NIES retrievals, then we use Eq. (15) of Connor et al. (2008):

$$\boldsymbol{X^m_{CO2}} = \boldsymbol{X^a_{CO2}} + \sum_j \boldsymbol{h_j}\, \boldsymbol{a_{co2,j}}\, (\boldsymbol{x_m} - \boldsymbol{x_a})_j \quad \textbf{(1)}$$

Here, $\boldsymbol{X^m_{CO2}}$ is the total column XCO_2 that the satellite would report if it observed the constructed ~~in situ~~ CO_2 profile x_m. We refer to $\boldsymbol{X^m_{CO2}}$ as "~~in situ~~observation-based XCO_2" (obs. XCO_2) in the following. $\boldsymbol{x_m}$ is the ~~in situ constructed~~ observation-based CO_2 profile (as a true profile). Extracted from the corresponding satellite retrievals, $\boldsymbol{X^a_{CO2}}$ is the a-priori XCO_2 of OCO-2, NIES, and ACOS, respectively, $\boldsymbol{h_j}$ the pressure weighting function, which is the change of atmospheric transmittance with respect to the pressure, $\boldsymbol{a_{CO2,\,j}}$ is the column averaging kernel, which represents the sensitivity profile to the total column amount, and $\boldsymbol{x_a}$ the a priori CO_2 profile. Comparison between monthly averages of the calculated ~~in situ~~obs. XCO_2 using $\boldsymbol{X^a_{CO2}}, \boldsymbol{h_j}, \boldsymbol{a_{CO2,\,j}}$, and $\boldsymbol{x_a}$ from the NIES and ACOS files showed agreement within 0.1 ± 0.1 ppm. Because the ACOS retrieval provides a higher number of valid data, we used the pressure levels and parameters from ACOS as representative for the calculation. After May 2016, we use the pressure grid and parameters from NIES due to the temporal limit of the ACOS v7.3 product.

It is noted that in our approach to obtain ~~in situ~~obs. XCO_2, the usage of model results above the TROPPB introduces little bias for two reasons. First, the CO_2 mixing ratio at these pressure levels varies much less than that in the middle and lower troposphere since there are no significant CO_2 sources and sinks in the stratosphere. Second, as mentioned earlier, the MIROC4-ACTM is among the best validated stratospheric models using high altitude balloon-borne measurements of SF_6 and CO_2-age-of-air (Patra et al., 2018), and in the upper troposphere and lower stratosphere using CONTRAIL observations (Bisht et al., 2021). Furthermore, in a sensitivity test, we compared XCO_2 derived from CO_2 profiles using the MIROC4-ACTM with that where the part of the CO_2 profile above the TROPPB was filled in by extrapolating the aircraft data up to 0.0128 hPa. The difference in XCO_2 was ~~as small as~~ only 0.2 ± 0.1 ppm on average.

4 Result and Discussion

4.1 Spatiotemporal variation of CO_2 seen by ship, aircraft, and satellite

Figure 3a-c presents the temporal variation of monthly average CO_2 mixing ratios obtained by ship and aircraft in three representative latitude ranges, namely the northern mid-latitudes (20° N–30° N), the equator region (0° N–10° N), and southern latitudes (20° S–10° S). Ship and aircraft data refer to lower and upper tropospheric CO_2 mixing ratios. The largest seasonal cycle of the CO_2 mixing ratio is seen in the northern hemisphere (NH) at 20° N–30° N. Average CO_2 mixing ratios of

402.9 ± 3.6 ppm and 401.2 ± 3.1 ppm at lower and upper troposphere, exceeded that from south of the equator by 4.5 ppm and 1.5 ppm, respectively. Maxima occur in April to May at sea -level, which is approximately 1 month earlier than in the upper troposphere (May to June). Minima seen in autumn show a greater temporal variability in the lower troposphere (August to October) than at about 10 km height (September). At 20° N–30° N, the peak-to-trough amplitudes of the seasonal cycles at sea level is 8.5 ± 0.9 ppm, and is ~2 ppm larger than the amplitudes in the upper troposphere (6.5 ± 0.6 ppm). Amplitudes decrease with latitude, showing similar values of about 4 ppm at the equator. In the southern hemisphere (SH), the amplitudes approach 0 at sea level **(Fig. 3c)**. In contrast, the upper troposphere shows two small peaks, one in June and one in November/December in 2014 and 2015, and additionally in April 2016. Seasonal cycles and decreasing amplitudes in the upper troposphere from North to South (~~76~~ ppm to ~~43~~ ppm) are similar to that observed by Matsueda et al. (2008). They found a decrease from 6 ppm at 30° N to 3 ppm at the equator over the same region between 2005 to 2007 using aircraft based flask samples. At sea -level, seasonal cycle amplitudes that decrease from about 8 ppm at 20° N–30° N to 3 ppm at the equator were reported by the global sampling network of the National Oceanic and Atmospheric Administration's Climate Monitoring and Diagnostics Laboratory (NOAA/CMDL) (Conway et al., 1994). The current observed characteristics are consistent with the previous long-term studies.

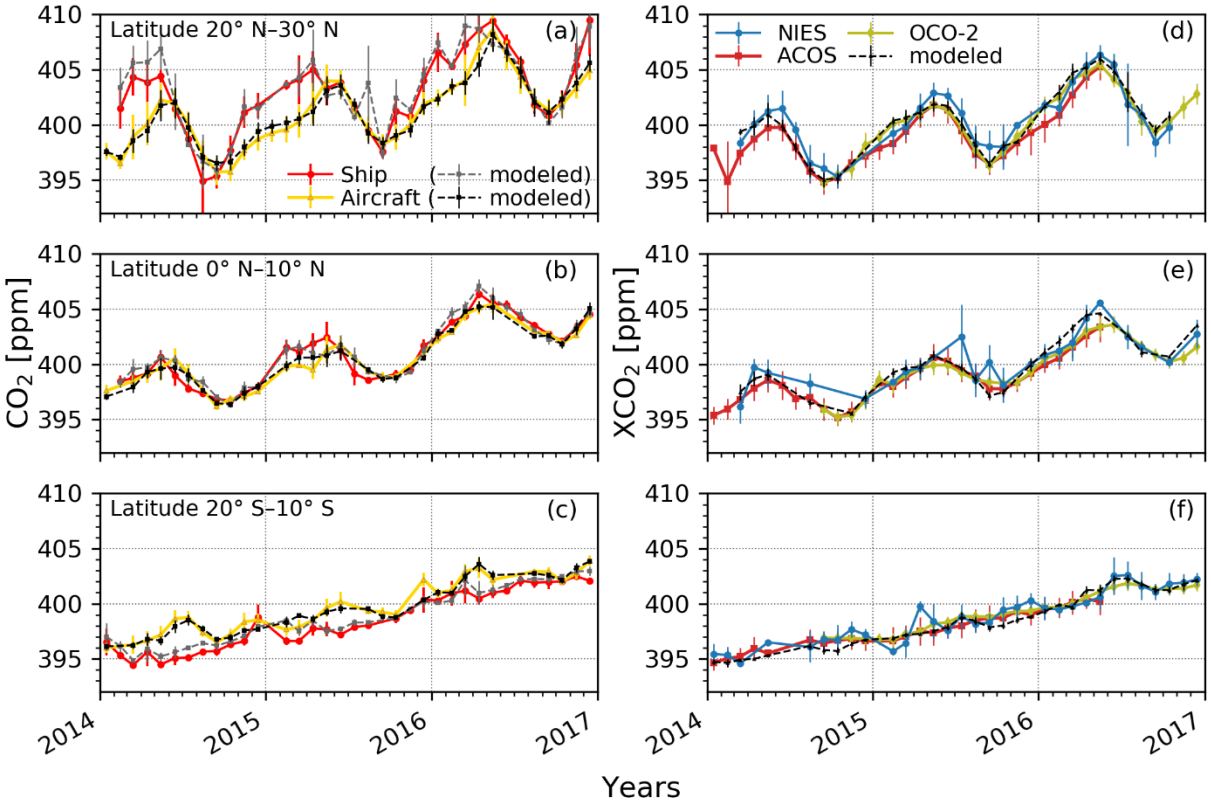

Figure 3. Temporal variation of the monthly average CO_2 mixing ratio obtained by ship (red) and aircraft (yellow) (left column), and the column averaged mixing ratios (XCO_2) from the NIES (blue), ACOS (red), and OCO-2 (olive) (right column) in three representative latitude ranges for the northern mid-latitudes a) and d), the equator region b) and e), and southern latitudes c) and f). Results of the ACTM are shown as dashed lines. Error bars represent the standard deviation of the monthly averages.

As the NH transitions from winter to spring, **Fig. 3a** reveals that the CO_2 mixing ratio increases rapidly at the surface, but only moderately at the upper troposphere, which results in a difference of up to 4 ppm. In 2014 and 2015, upper tropospheric peak values show a delay of 1 month, which is not seen in 2016, likely due to year-to-year variations. Similar observation have been made previously over the northern Pacific (Miyazaki et al., 2008; Nakazawa et al., 1991) and attributed to the response of the terrestrial carbon metabolism of the NH (China, Korea, Japan) and predominant northwesterly airmass transport (Umezawa et al., 2018). Specifically, low net primary productivity (NPP) and leaf litter decomposition in autumn to winter is linked to a net carbon release from the terrestrial ecosystem and subsequent increase in the CO_2 mixing ratio at the lower troposphere, which persists until spring. Vertical mixing mitigates the altitude dependent CO_2 gradient with a time offset of about 5 months. In spring to summer, high NPP rates substantially removes CO_2 from the atmosphere. At that season, strong convection, associated with significant uplift of low-CO_2 air masses, results in a well-mixed troposphere (Miyazaki et al., 2008; Nakazawa et al., 1991; Niwa et al., 2011). The flux footprints on upper tropospheric CO_2 is generally much wider compared to that near the surface at all latitudes, resulting in a smoother vertical gradients and smaller seasonal cycle amplitudes at higher altitudes.

Figure 3d-f presents the temporal variation of column averaged mixing ratios of CO_2 (XCO_2) retrieved by NIES, ACOS, and OCO-2. The number of valid bias corrected XCO_2 retrievals by NIES are less than 25 % of that by ACOS with good quality flag. Seasonal patterns of all retrievals were similar in the NH, showing peaks in late spring/early summer (May to June), and minima in autumn (September to October). While peaks of XCO_2 by NIES are higher by 1 to 3 ppm, ACOS and OCO-2 values agree within 1 ppm (**Figs. 3d and 3e**). The largest amplitudes of ACOS and OCO-2 at 20° N–30° N (5 to 6 ppm) are approximately 2 ppm smaller than those of NIES (6 to 8 ppm). Southwards, the strong seasonal cycle decreases, and disappears in the SH, similar to observations made by in situ measurements at sea level. The NIES XCO_2 product shows substantial scatter and limited valid data each month at lower latitudes, unlike ACOS and OCO-2 (**Figs. 3e and 3f**). Differences in retrieval algorithms can explain discrepancies in the XCO_2 (Reuter et al., 2013), while the reduced number of data points of NIES are likely due to stricter quality filters. The results imply that seasonal variations of CO_2 at lower latitudes are better represented by the ACOS/OCO-2 retrieval algorithm.

Table 1. Root-mean-square error (RMSE), and average difference and standard deviation between the retrievals from aircraft, ship, satellite and the corresponding results from the ACTM at different latitude ranges between 2014 and 2017.

			RMSE		
Latitude	**Aircraft**	**Ship**	**NIES**	**ACOS**	**OCO-2**
20° N–30° N	0.54	1.26	0.93	1.09	0.44
0° N–10° N	0.44	0.68	1.14	0.93	0.93
20° S–10° S	0.55	0.63	0.86	0.54	0.56

	Difference measured in situ or/satellite XCO_2 − ACTM (ppm)				
Latitude	**Aircraft**	**Ship**	**NIES**	**ACOS**	**OCO-2**
20° N–30° N	0.00 ± 0.54	−0.41 ± 1.19	0.16 ± 0.92	−0.81 ± 0.72	−0.30 ± 0.32
0° N–10° N	0.01 ± 0.44	−0.20 ± 0.65	0.17 ± 1.13	−0.58 ± 0.72	−0.51 ± 0.78
20° S–10° S	0.13 ± 0.54	−0.40 ± 0.48	0.33 ± 0.80	0.15 ± 0.52	0.20 ± 0.52

Figure 3 also presents the simulated XCO_2, sea-level CO_2 mixing ratios, and upper troposphere CO_2 mixing ratios, calculated by the MIROC-4-ACTM. Best agreement is found between the model results in the upper troposphere and the aircraft observations (RMSE 0.51 ± 0.05, average difference 0.05 ± 0.06) (**Table 1**). The largest discrepancy to the model results occur for the ship observations at northern midlatitudes (RMSE 1.26, difference 0.41 ± 1.19), likely due to the large gradients and variations of CO_2 concentrations typically found at this latitude range at sea-level. The coarse horizontal resolution of the model is not adequate to represents observations near source regions. The RMSE of the difference between satellite XCO_2 and the MIROC-4-ACTM ranges from 0.44 to 1.14, which may result both from the higher uncertainties of the simulations at sea-level, and the uncertainties in the satellite retrievals. OCO-2 v9r shows systematically higher RMSE around the equator at 0° N–10° N, relative to the 20° N–30° N and 10° S–20° S region.

4.2 Latitudinal variations of CO_2 seen by ship, aircraft, and satellite

Figure 4a-c displays the latitudinal distribution of the CO_2 mixing ratio of ship and aircraft for three selected months in 2015, which are representative for different latitudinal CO_2 gradients in the troposphere. From North towards the equator, the negative tropospheric CO_2 gradient decreases rapidly, especially in spring (March) and autumn (October) (**Figs. 4a and 4c**). Around the equator, ship and aircraft mixing ratios agree within 0.2 ± 0.8 ppm. In the SH, the gradient is reversed, showing upper tropospheric CO_2 mixing ratio to be larger by 1.4 ± 0.9 ppm, especially during NH spring to summer (**Fig. 3c, Fig. 4b**). Previous model studies, which included aircraft observations, explain the atmospheric CO_2 characteristics south of the equator by meridional transport processes (Miyazaki et al., 2008; Niwa et al., 2011). Our current ACTM forward simulations reveal in particular that CO_2, which is strongly emitted during winter to spring (December to May) over NH land, causes a strong meridional CO_2 gradient at sea level, and the CO_2 rich air is transported towards the equator (**Fig. A2**). In NH summer (June to August), the meridional gradient is substantially weakened due to the seasonal CO_2 sink at northern midlatitudes (**Fig. 4b, Figs. A2f-h**). At the upper troposphere, meridional gradients are absent during autumn (September-November) (**Fig. 4c, Figs. A2i-k**) and gradients are weak in winter (December to February) (**Figs. A2l-b**), but increase towards summer due to vertical mixing of CO_2 rich air from the surface at northern midlatitudes (**Fig. 4a, Figs. A2c-e**). Near the equator, uplift by convection increase the CO_2 mixing ratio in the middle and upper troposphere in all seasons. In the SH, strong meridional transport from the NH to the SH occurs only from late spring to early summer in the upper troposphere during which time the

CO_2 mixing ratio in the upper troposphere exceeds that at the sea-surface (**Fig. 4b**). Furthermore, CO_2 uptake by the Southern Pacific and southern hemispheric land vegetation decrease CO_2 at sea-level. The current in situ observations confirm the inter-hemispheric transport mechanism of CO_2.

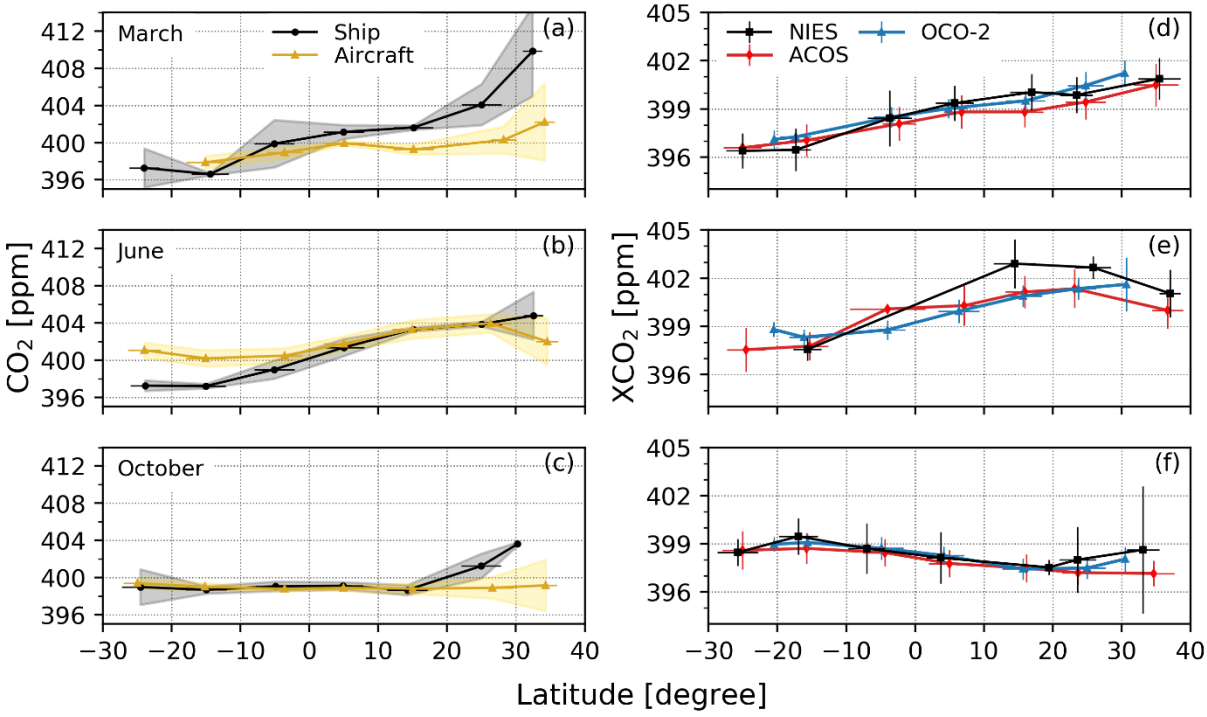

Figure 4. Latitudinal distribution of the CO_2 mixing ratio obtained by ship (black) and aircraft (yellow) (left column), and of XCO_2 obtained by NIES (black), ACOS (red), and OCO-2 (blue) (right column) for three selected months in 2015, which are representative for different latitudinal CO_2 gradients in the troposphere: March a) and d), June b) and e), and October c) and f). Shaded areas are the standard deviation of the monthly average CO_2 mixing ratios. Error bars show the standard deviation of the monthly averaged XCO_2, and of the location within each latitude box.

Figure 4d-f shows the latitudinal distribution of XCO_2 retrieved by NIES, ACOS, and OCO-2. In spring, maximum values appear in the NH and minima in the SH (**Fig. 4d**). In autumn, the locations of the maxima and minima are reversed between NH and SH (**Fig. 4f**). In summer (June), the maxima occur at 10° N–20° N (**Fig. 4e**), which is the result of substantial carbon removal by high NPP at higher latitudes (30° N–40° N) as described above. At that transition point, XCO_2 of NIES exceeds that of ACOS and OCO-2 by about 2 ppm. The in situ and satellite observations reveal the complex CO_2 fluxes and transport processes. The results demonstrate that measuring upper and lower tropospheric CO_2 mixing ratios simultaneously is important to better understand CO_2 fluxes, which is necessary to further improve atmospheric chemistry transport models. The

consistency of the satellite XCO_2 with in situ observations will be evaluated by comparison with the corresponding ~~in situ~~obs. XCO_2 values in the following section.

4.3 Evaluation of seasonal and interannual changes of satellite XCO_2 by combined ship and aircraft observations

Figure 5a-c shows the temporal variation of the satellite and obs.~~in situ derived~~ XCO_2, and the difference between ~~in situ derived~~obs. and satellite XCO_2 in **Figs. 5d-f**. The uncertainties of the obs. XCO_2 dataset are estimated to be 0.62 ± 0.01 ppm on average, which is derived from the ±2 ppm variation in the observation-based CO_2 profile at 2 km above sea level (**section 3.2**).

In all latitudes, obs.~~in situ~~ and satellite XCO_2 show an overall significant positive correlation (R^2: NIES = 0.84 ± 0.02, ACOS = 0.74 ± 0.0~~7~~8, OCO-2 = 0.8~~1~~2 ± 0.0~~4~~5) (**Table 2**). However, in the NH, satellite retrievals are negatively biased by up to 1.6 ± 0.6 ppm (ACOS) at 20° N–30° N (**Figs. 5a and 5d, Table 3**). The smallest average bias is found for NIES, likely due to the stricter quality filters as discussed in **section 4.1**. While ACOS and OCO-2 show rather a systematic offset, the NIES retrieval seems to be more noisy (**Figs. 5d and 5e, Table 3**). The root-mean-square error (RMSE) of the difference between ~~in situ~~obs. XCO_2 and satellite XCO_2 is 1.06, 1.26, and 1.70 for NIES, OCO-2, and ACOS respectively, and decreases by 40% (0.5~~3~~6 ppm) on average between the northernmost and southernmost regions (**Table 2**). Agreement within 1 ppm on average is found in the SH (**Figs. 5c and 5f**). The uncertainties of the differences between obs. XCO_2 and the satellite retrievals are large. However, the comparison indicates whether the results of the current satellite retrievals tend to show a systematic positive or negative offset (ACOS, OCO-2), or rather a random discrepancy. This comparison is of importance for revising the retrieval algorithm in future.

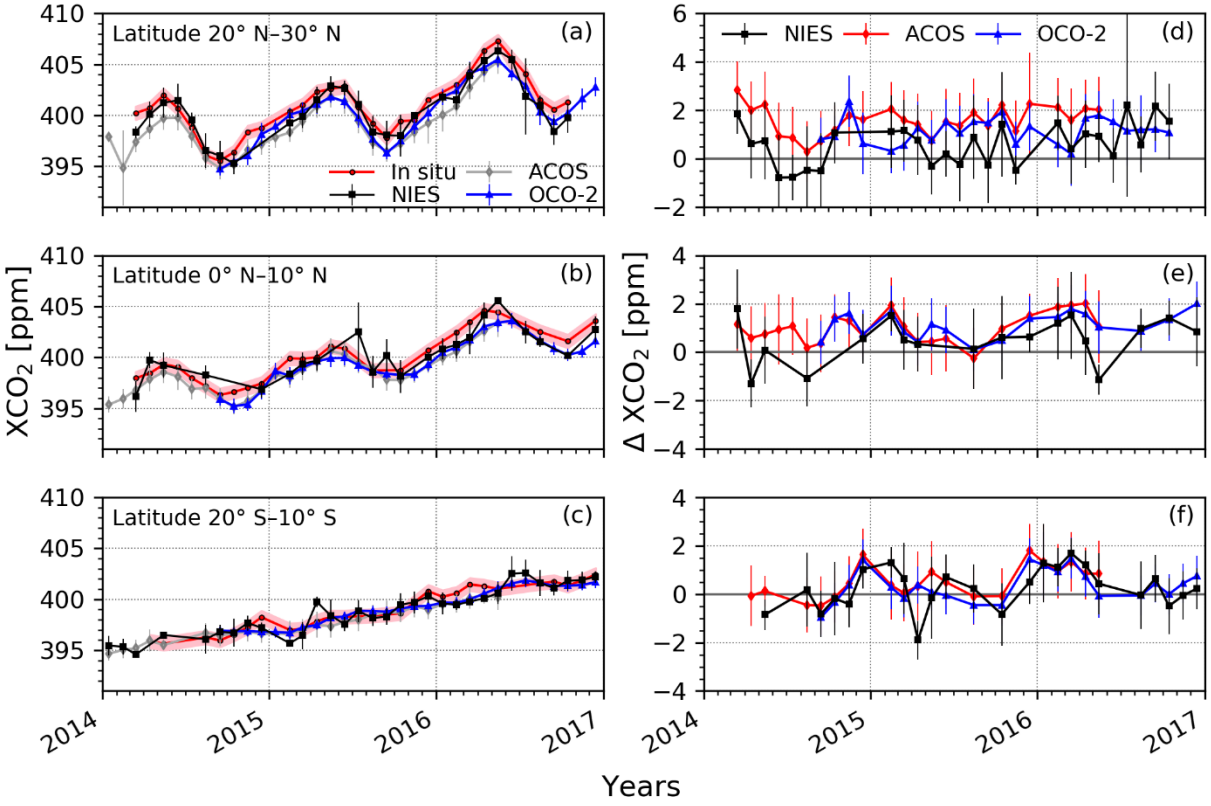

Figure 5. Temporal variation of the satellite derived XCO_2 obtained by NIES (black), ACOS (grey), and OCO-2 (blue) in comparison with the ~~in situ~~obs. XCO_2 (red) (left column), and the difference between obs. XCO_2~~in situ derived~~ and NIES (black), ACOS (red), and OCO-2 (blue) (right column) for three selected latitude boxes. Red shaded areas are the uncertainty of the ~~in situ~~obs. XCO_2 derived from the ±2 ppm variability in the ~~in situ constructed~~observation-based CO_2 profile at ~850 hPa. Error bars show the standard deviation of the monthly averaged XCO_2.

Table 2. Coefficient of determination (R^2) and root-mean-square error (RMSE) between ~~in situ~~obs. XCO_2 and satellite XCO_2 retrievals from GOSAT (NIES, ACOS) and OCO-2 at different latitude ranges between 2014 and 2017.

	R^2			RMSE		
Latitude	**NIES**	**ACOS**	**OCO-2**	**NIES**	**ACOS**	**OCO-2**
20° N–30° N	0.86	0.64	0.81	1.06	1.70	1.26
0° N–10° N	0.81	0.76	0.76	1.02	1.17	1.23
20° S–10° S	0.854	0.821	0.887	0.847	0.7983	0.730

Table 3. Average (Avg.) difference and the standard deviation (SDtd.) between ~~in situ~~obs. and satellite XCO_2 from GOSAT (NIES, ACOS) and OCO-2 of each latitude range between 2014 and 2017.

	difference ~~in situ~~obs. XCO_2 – satellite XCO_2					
Latitude	**Avg. NIES**	**SDtd.**	**Avg. ACOS**	**SDtd.**	**Avg. OCO-2**	**SDtd.**
20° N–30° N	0.61	0.87	1.60	0.59	1.14	0.52
0° N–10° N	0.51	0.87	1.00	0.60	1.12	0.52
20° SN ~~–~~ 10° S	0.2~~3~~0	0.841	0.48~~5~~1	0.6~~6~~3	0.314	0.63~~5~~

Figure 6 displays the latitudinal gradients and the gradient of the difference between ~~in situ~~obs. and satellite XCO_2 for the three selected months March, June, and October in 2015 as described above (**section 4.2**). It reveals that generally, the largest differences in the NH coincide with the latitude of the monthly XCO_2 maxima. Namely, at 30° N–40° N in spring and autumn with up to 3 ppm (between ~~in situ~~obs. XCO_2 and ACOS in March) (**Figs. 6a and 6d**) and in June at 10° N–20° N with a discrepancy of up to 2 ppm (between ~~in situ~~obs. XCO_2 and OCO-2) (**Figs. 6b and 6e**). The difference might be caused by uncertainties in the obs. XCO_2 due to the variability of the TROPPB (**section 3.2**). However, the uncertainty in the TROPPB results in a difference in the obs. XCO_2 of only 0.03 ± 0.06 ppm on average. This leads to a total estimated error of 0.7 ppm considering the uncertainty of 0.62 ± 0.01 ppm derived from the ±2 ppm variation in the observation-based CO_2 profile at 2 km above sea level (**section 3.2**). It is known that ~~A~~atmospheric CO_2 mixing ratios in midlatitudes are characterized by high spatiotemporal variability. Therefore, the observed discrepancies in the NH may arise from differences in sample numbers, location and time within each month and latitude-longitude range. In particular, the largest uncertainty in the ~~in situ~~obs. XCO_2 likely results from the constructed CO_2 profile in the mid-troposphere, as no observational constraints are available for that part of the atmosphere and simply a linear interpolation between the ship and aircraft data was assumed (**section 3.2**).

However, **Fig. 3a** reveals that ship and aircraft CO_2 mixing ratios are very similar in the second half of each year. Model results of the MIROC~~-~~4~~-~~ACTM confirm vertically uniform CO_2 profiles during that period, which lie within the uncertainty range of the ~~in situ constructed~~observation-based profiles (**Fig. A3**). Niwa et al. (2011) found similar straight vertical profiles between June and September in East Asia, based on aircraft observations and model results. Furthermore, the maximum bias due to errors in the MIROC4-ACTM stratospheric CO_2 profile (0.9 ppm) is smaller than the average difference of 1.2 ± 0.4 ppm between the obs. XCO_2 and satellite observations of ACOS and OCO-2 between June and September (**section 3.2**). Hence, even though no assumption was necessary at that period, the negative bias persists (**Fig. 5d, Fig. 6e**), which indicates that the difference between ~~in situ~~obs. and satellite XCO_2 can be linked to measurement uncertainties of the satellites.

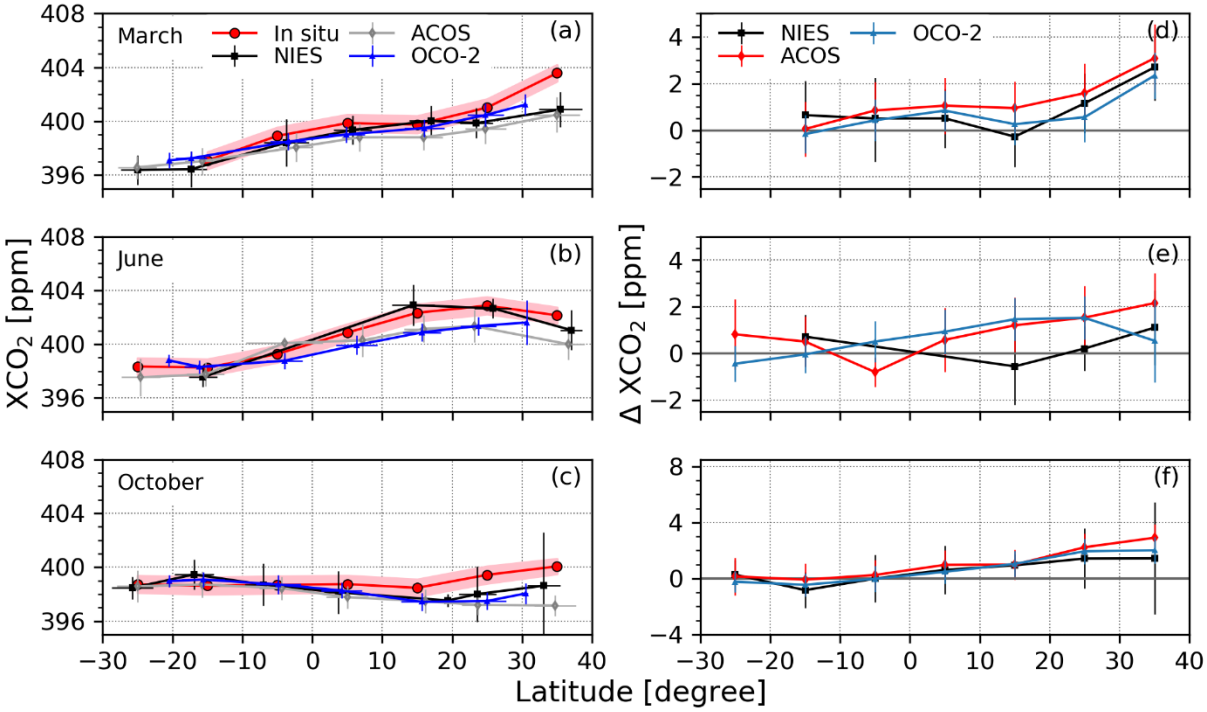

Figure 6. Latitudinal gradients of ~~in situ derived~~obs. XCO_2 (red) in comparison with the satellite XCO_2 from NIES (black), ACOS (grey), and OCO-2 (blue) (left column), and the difference between the ~~in situ derived~~obs. XCO_2 and NIES (black), ACOS (red), and OCO-2 (blue) (right column) for three selected months, March a) and d), June b) and e), and October c) and f) in 2015. Red shaded areas are the uncertainty of the ~~in situ~~obs. XCO_2 derived from the ±2 ppm variability in the ~~in situ constructed~~observation-based CO_2 profile at ~850 hPa. Error bars show the standard deviation of the monthly averaged XCO_2 and of the location within each latitude box.

The peak values in the carbon cycle represent the turning points between predominant CO_2 sources in boreal winter, and sinks in summer and therefore, are important to constrain changes in the seasonal and interannual variation of the carbon cycle. **Figures 5a and 5b** reveal that maxima and minima generally agree. However, small positive phase shifts of about one month are occasionally observed (2014, 20° N–30° N: maximum of NIES in June; 2014, 10° N–20°N minima of ACOS and OCO-2 in October; 2016, 10° N–20°N: maximum of OCO-2 in June). Long-term measurements (1984 to 2013) observed maxima usually in May and minima in late September in the upper troposphere of the northern West Pacific (Matsueda et al., 2008, 2015). Surface data (between 1987 and 2017) reported maxima in early May and minima in early September over the same region (World Data Centre for Greenhouse Gases (WDCGG) of the World Meteorological Organization (WMO)). The consistency with long-term studies support the correctness of the ~~in situ~~ obs. XCO_2, which implies that satellite XCO_2 sometimes show a delayed response to CO_2 changes~~.~~, which might be caused by remaining uncertainties introduced by limitations in the retrieval algorithms and have not been previously identified due to the lack of validation data over the open ocean.

To explore year-to-year changes in the increase of XCO_2, the mean values of the three consecutive highest monthly averages during spring of each year are compared (**Table 4**). Three-month averages around the peak values are chosen due to the limited data, although usually longer time-periods are needed for that growth calculation. From 2014 to 2015, ~~in situ~~obs. and satellite XCO_2 increased by 1.61 ± 0.24 ppm yr^{-1} on average ~~less than 2 ppm yr^{-1}~~ at 20° N–30° N **(Table 4, Fig. 5a)**. In contrast, a significant increase of 3.84 ± 0.65 ppm yr^{-1} is observed by ~~in situ~~obs. XCO_2 from 2015 to 2016. The average increase of the mean values of all satellite retrievals is 3.39 ± 0.03 ppm yr^{-1}. This~~, which is by ~10% larger than that observed by satellites (3.39 ± 0.03). The~~ rapid increase is also seen near the equator, where the increase of the obs. XCO_2 is significantly higher than that of ACOS and OCO-2 (two-sided t-test, significance level α=0.05). ~~simultaneously~~Simultaneously, ~~with~~ a larger negative bias of the satellite XCO_2 in 2016 as compared to the previous years is observed **(Figs. 5b and 5e)**.

Table 4. Increase of XCO_2 between peaks of consecutive years and the standard error of the difference seen by obs.~~in situ~~ and satellite XCO_2 of GOSAT (NIES, ACOS) and OCO-2 between 2014 and 2017. Peak values are defined as mean of the three consecutive highest monthly averages during spring of each year. In 2016, the mean of ACOS and that of ~~in situ~~obs. XCO_2 at 0° N–10° N is based on 2 months due to limited data. "–" indicates missing data. The right column shows the average increase of all satellite means and its standard deviation.

	~~In situ~~Obs. XCO_2 (ppm yr^{-1})	NIES (ppm yr^{-1})	ACOS (ppm yr^{-1})	OCO-2 (ppm yr^{-1})	Avg. all satellites (ppm yr^{-1})
			20° N–30° N		
2014–2015	1.45 ± 0.63	1.42 ± 0.60	1.95 ± 0.54	–	1.68 ± 0.26
2015–2016	3.84 ± 0.65	3.37 ± 0.43	3.43 ± 0.40	3.36 ± 0.38	3.39 ± 0.03
			0° N–10° N		
2014–2015	1.72 ± 0.22	–	1.99 ± 0.30	–	–
2015–2016	3.87 ± 0.09	–	2.82 ± 0.37	3.52 ± 0.16	3.17 ± 0.35

The larger increase between 2015 and 2016 is likely driven by the strong El Niño in 2015. Matsueda et al. (2008) reported a mean CO_2 growth rate of 1.7 to 1.8 ppm yr^{-1} in 1993 to 2005. However, between 1997 to 1998, they found a significantly enhanced growth rate of about 3 ppm yr^{-1}, which they linked to a strong El Niño year (Matsueda et al., 2002, 2008). Indeed, it is well documented that the interannual variation in the growth rate of CO_2 is closely linked to the El Niño–Southern Oscillation (ENSO), which affects the carbon cycle though changes in the atmospheric and ocean circulation (e.g., Bacastow, 1976; Keeling, C. D.Revelle, 1985; Kim et al., 2016; Patra et al., 2005; Wang et al., 2013; Zeng et al., 2005). Particularly, the increase of CO_2 was attributed to a decrease in the NPP, increased soil respiration, and enhanced fire emissions related to low precipitation and high temperatures (Liu et al., 2017). Recent model results found that the maximum CO_2 growth rate appears several months after the El Niño peak as response to the low NPP (Kim et al., 2016). In fact, the maximum increase observed in this study occurred in NH spring, after the peak of the 2015 El Niño in November/December **(Figs. 5a and 5b)**.

Opposite to the strong increase, ~~in situ~~obs. XCO_2 shows no increase between March and April around the equator in 2015 (**Fig. 5b**). One month earlier (February), a reduction in XCO_2 is seen by ACOS and OCO-2. It has been argued that the upwelling of carbon rich water to the surface at the equator is suppressed in the eastern and central Pacific Ocean during El Niño (Feely et al., 2002; Keeling, C. D.Revelle, 1985), which subsequently leads to an initial negative CO_2 anomaly over that region (Rayner et al., 1999). Coincident timing of the observed anomalies with different phases of the El Niño suggest that the ocean and terrestrial response to the event affect the atmospheric CO_2 mixing ratio even at the study region at 140° E to 160° E. Supportive to this interpretation, Chatterjee et al. (2017) found a negative anomaly in atmospheric CO_2 concentrations over the so-called Niño 3.4 region (120° W–170° W) between March and July 2015 in the OCO-2 retrievals. Consequently, ACOS and OCO-2 reflect the negative anomaly of CO_2 of the first phase of the El Niño, whereas in the second phase, the response of the atmospheric CO_2 mixing ratio to the event is better represented by the higher growth rate of the ~~in situ~~obs. XCO_2. Given the uncertainties associated with the negative CO_2 anomaly observed at the study region, the result therefore suggests that, compared to satellite observations, ~~in situ~~obs. XCO_2 sometimes show a higher sensitivity to year-to-year changes in the atmospheric CO_2 mixing ratio.

5 Conclusions

The current study indicates that seasonal, latitudinal and interannual variation of atmospheric CO_2 mixing ratios over the open ocean can be accurately determined by ~~in situ derived~~observation-based column average CO_2 mixing ratios, defined as ~~in situ~~obs. XCO_2. The sensitivity of the ~~in situ~~obs. XCO_2 dataset to year-to-year variations was demonstrated on the distinct ocean and terrestrial responses to the 2015–2016 El Niño event around the equator. Namely, a stagnation in the springtime increase during the early stage of the El Niño event was linked to reduced CO_2 outgassing from the ocean, and a substantial increase to the later stage, reflecting the increase of CO_2 emissions from the terrestrial ecosystem.

The evaluation of three different satellite retrievals (ACOS, NIES, OCO-2) by the ~~in situ~~obs. XCO_2 revealed similar seasonal pattern (R^2 = 0.64–0.87). However, a negative bias of 1.12 ± 0.40 ppm on average and higher difference in the northern (NH) than in the southern hemisphere (SH) were attributed to measurement uncertainties of the satellites. Compared to ACOS and OCO-2, the NIES retrieval showed higher accuracy in the northern hemispherical midlatitudes. At low latitudes, NIES retrievals show substantial scatter and very few valid data points. ACOS and OCO-2 provide a more reliable analysis of carbon cycles at these latitudes. The seasonal cycle of all retrievals occasionally showed a positive phase shift of one month relative to the ~~in situ~~obs. XCO_2 at different times of year. In some cases, the representation of year-to-year variations in atmospheric CO_2 mixing ratios is more distinct in the ~~in situ~~obs. XCO_2 values as compared to the satellite estimates and therefore, are suggested to be sometimes of higher sensitivity. Hence, the result indicates that even if the retrievals complement each other, measurement uncertainties remain, which limit the accurate interpretation of spatiotemporal changes in CO_2 fluxes by satellites alone. These uncertainties might be introduced by limitations in the retrieval algorithms and have not been previously identified due to the lack of validation data over the open ocean.

Advanced observations like those from GOSAT-2 and improvements in retrieval algorithms like those from ACOS version 9, and OCO-2 version 10, increase the number of valid data points at lower latitudes and reduce uncertainties. An initial comparison of the ~~in situ~~obs. XCO_2 dataset with ACOS v9~~r~~ revealed a decrease of the negative bias by more than 50% on average ~~at northern midlatitudes~~ as compared to ACOS v7.3 (**Fig. A1**), and the comparison with OCO-2 v10, a decrease of the average bias by more than 90% as compared to OCO-2 v9r (**Fig. A2**). This example highlights the utility of the ~~in situ~~obs. XCO_2 dataset as a reference for satellite derived XCO_2 estimates and to clarify the impacts of changes between different versions of retrieval algorithms.

Our study provides a short-term perspective on the great potential of the new bottom-up approach which can help to understand changes in the carbon cycle in response to global warming and to interpret their contribution to atmospheric CO_2 growth. We propose that a long-term XCO_2 dataset based on co-located CO_2 measurements by commercial ships and aircraft can augment TCCON data for validating XCO_2 estimates from satellites over the open ocean. To accomplish this objective, these commercial ship and aircraft measurements should be expanded and must be sustained for the foreseeable future.

Appendix A:

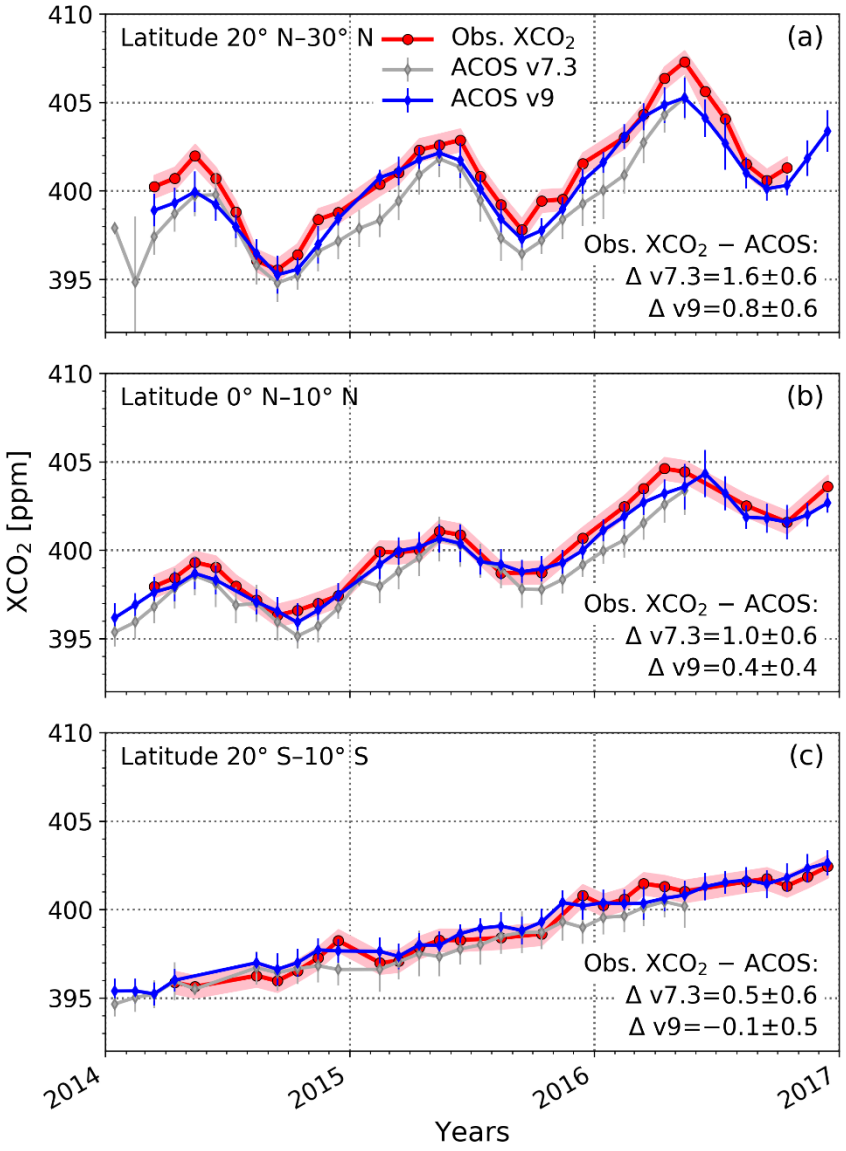

Figure A1. Comparison of the temporal variation of ~~in situ~~obs. XCO_2 (red) with XCO_2 derived from ACOS v7.3 (grey) and ACOS v9 (blue) for three selected latitude ranges. Red shaded areas are the uncertainty of the ~~in situ~~obs. XCO_2 derived from the ±2 ppm variability in the ~~in situ constructed~~observation-based CO_2 profile at ~850 hPa. Error bars show the standard deviation of the monthly averaged XCO_2.

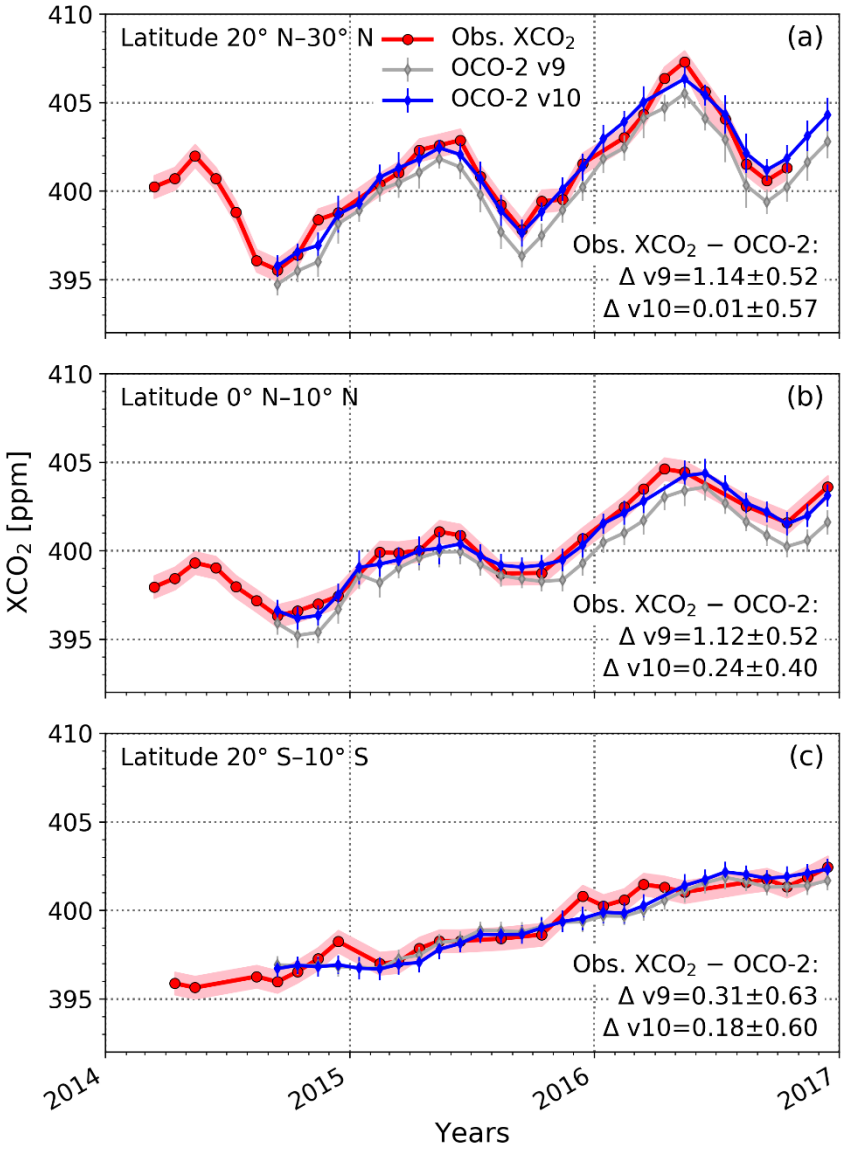

Figure A2. Comparison of the temporal variation of obs. XCO_2 (red) with XCO_2 derived from OCO-2 v9 (grey) and OCO-2 v10 (blue) for three selected latitude ranges. Red shaded areas are the uncertainty of the obs. XCO_2 which was obtained from the ±2 ppm variability in the observation-based CO_2 profile at ~850 hPa. Error bars show the standard deviation of the monthly averaged XCO_2.

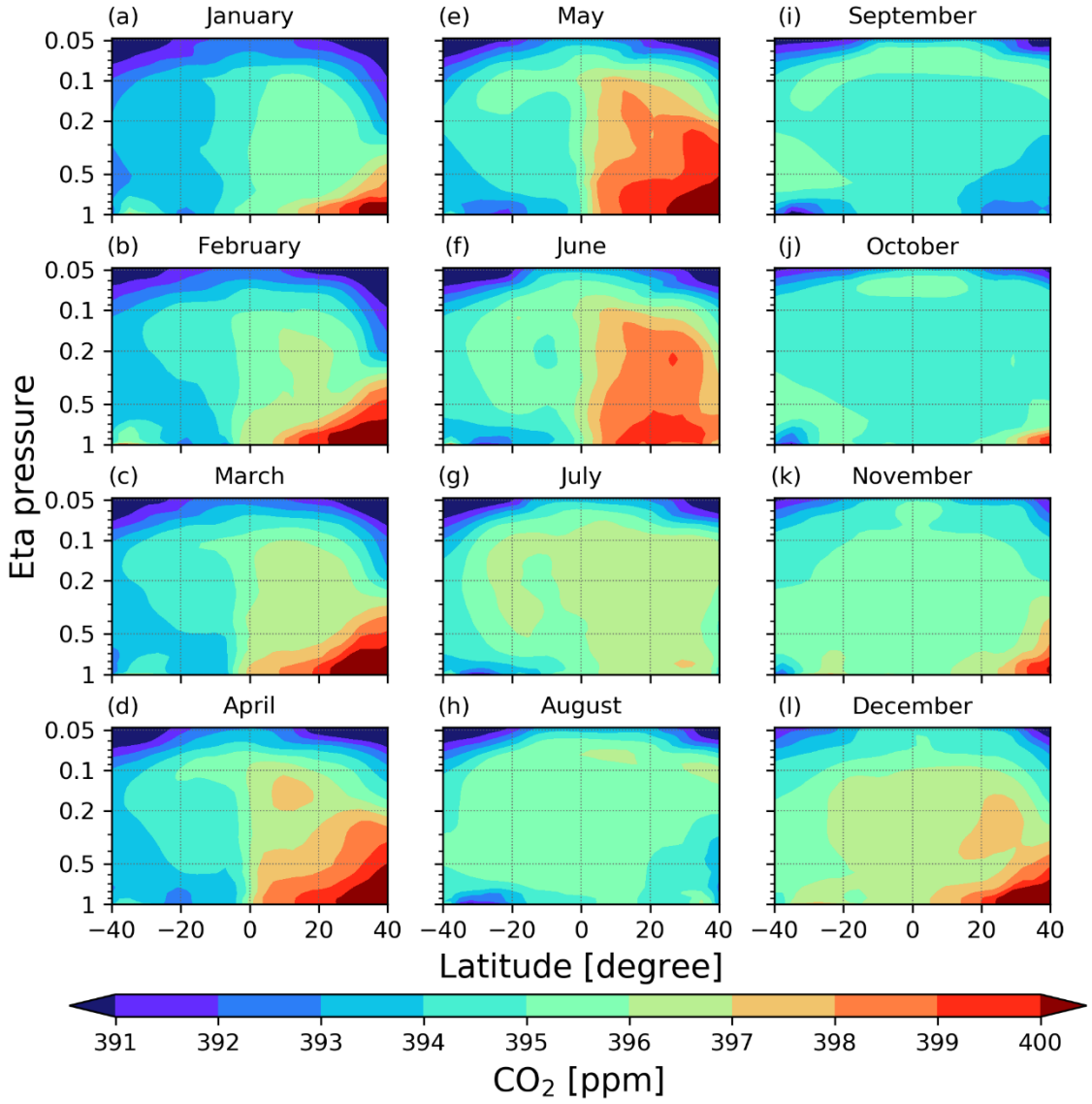

Figure A32. Latitude-pressure distribution of the inversion of the CO_2 mixing ratio at longitude 146° E in 2015, obtained from ACTM forward simulations.

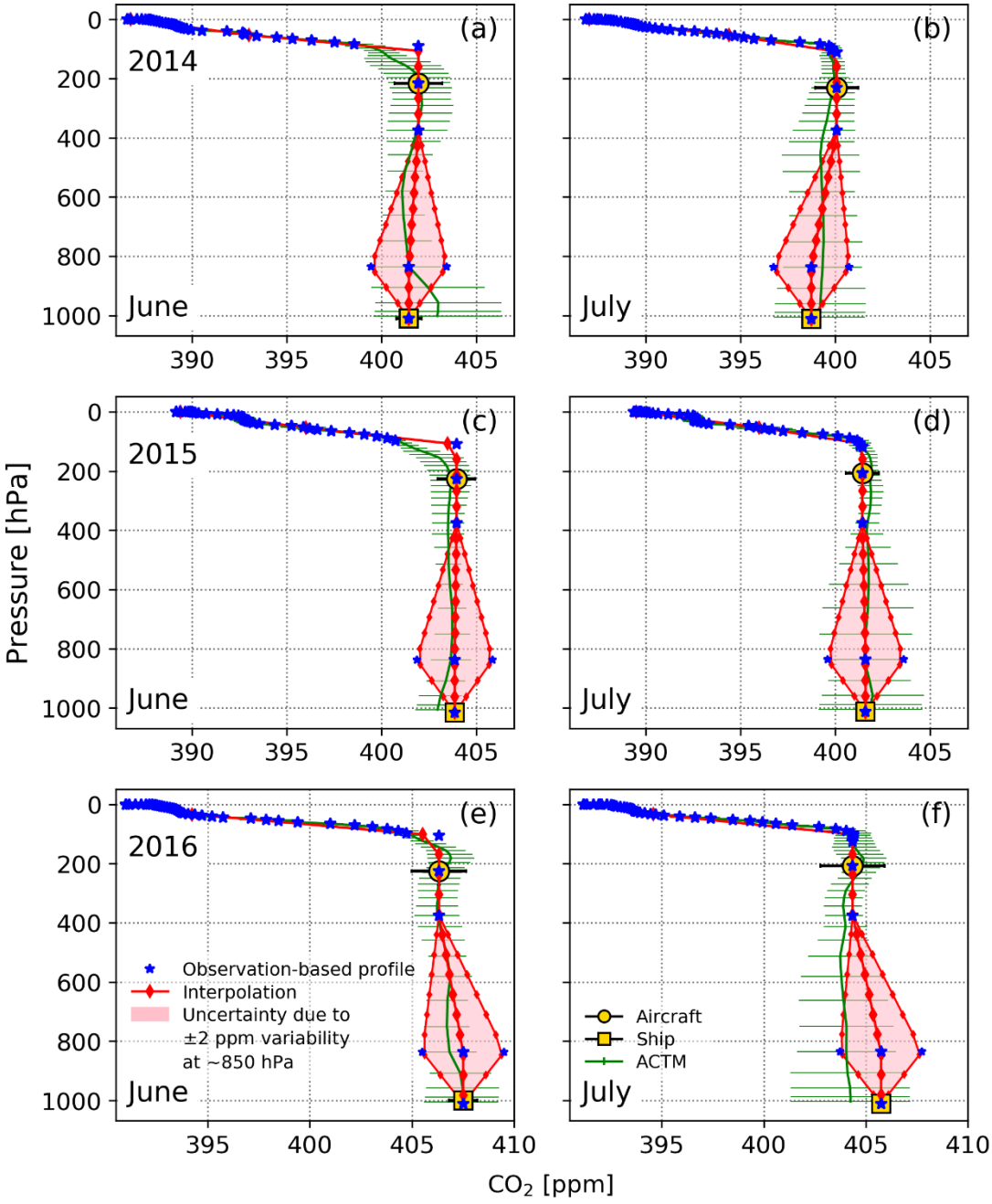

Figure A~~3~~4. Observation-based ~~In-situ constructed~~ CO_2 profiles (blue) obtained by using ship (SOOP) and aircraft (CONTRAIL) data (yellow), together with the results of the ACTM (green), and the interpolation (red) for the month June and July in 2014 a), b), 2015 c), d), and 2016 e), f) at the latitude range 20° N–30° N.

Data availability. The OCO-2 data presented in this manuscript are available from the NASA Goddard GES DISC at https://disc.gsfc.nasa.gov/datasets/OCO2_L2_Lite_FP_9r/summary (OCO-2 Science Team/Michael Gunson, Annmarie Eldering, 2018). ACOS data are available at https://disc.gsfc.nasa.gov/datasets/ACOS_L2_Lite_FP_9r/summary (OCO-2 Science Team/Michael Gunson, Annmarie Eldering, 2019), and at https://disc.gsfc.nasa.gov/datasets/ACOS_L2_Lite_FP_7.3/summary (OCO-2 Science Team/Michael Gunson, Annmarie Eldering, 2016). GOSAT data are available from the GOSAT Project website of the National Institute for Environmental Studies ("NIES") at https://data2.gosat.nies.go.jp/index_en.html, accessed: [4/28/2020]. SOOP data are available at http://soop.jp/, accessed: [9/26/2019]. The CONTRAIL CME CO_2 data are available on the Global Environmental Database of the Center for Global Environmental Studies of NIES (https://doi.org/10.17595/20180208.001). The CONTRAIL data are also available from the ObsPack data product (http://www.esrl.noaa.gov/gmd/ccgg/obspack/) and the World Data Center for Greenhouse Gases (https://gaw.kishou.go.jp/).

Supplementary data. Supplementary information and data accompany this article.

Author Contributions. The study was designed by H.T. Data analyses were made by A.M., and extensive discussions were made by A.M., H.T., T.S., T.M., P.P., J.L., and D.C. The paper was written, edited, and proofed by all the authors.

Competing Interests. The authors declare that they have no competing interests.

Acknowledgements. We are grateful to Dr. Naveen Chandra, NIES for providing CO_2 inversion fluxes that are used for simulating atmospheric concentration by ACTM. We also would like to thank the anonymous reviewers for valuable comments and suggestions improving the paper.

Financial support was given by multiple grants: the Global Environmental Research Coordination System from the Ministry of the Environment, Japan (E1851, E1253, E1652, E1151, E1951, E1451, E1751, E1432), and the Environmental Research and Technology Development Fund (ERTDF) from the Ministry of the Environment, Japan (grant no. 2-1803. JPMEERF20182003).

The authors acknowledge the satellite data infrastructure for providing access to the GOSAT NIES, the GOSAT ACOS and the OCO-2 data used in this study. This research is a contribution to the Research Announcement on GOSAT series joint research, entitled “Combined cargo-ship and passenger aircraft observations-based validation of GOSAT-2 GHG observations over the open oceans”, and to the Greenhouse Gas Initiative of the Atmospheric Composition Virtual Constellation (AC-VC)

of the Committee on Earth Observation Satellites (CEOS). We thank the WDCGG (World Data Centre for Greenhouse Gases) for providing CO_2 reference data of the Pacific Ocean from the NOAA GMD Carbon Cycle Cooperative Global Air Sampling Network, 1968-2018 (Principal investigators include Ed Dlugokencky (NOAA)). Part of this work was conducted at the Jet Propulsion Laboratory, California Institute of Technology, under contract to the National Aeronautics and Space Administration. Government sponsorship acknowledged.

References

Bacastow, R. B.: Modulation of atmospheric carbon dioxide by the Southern Oscillation, Nature, 261(5556), 116–118, doi:10.1038/261116a0, 1976.

Basu, S., Guerlet, S., Butz, A., Houweling, S., Hasekamp, O., Aben, I., Krummel, P., Steele, P., Langenfelds, R., Torn, M., Biraud, S., Stephens, B., Andrews, A. and Worthy, D.: Global CO_2 fluxes estimated from GOSAT retrievals of total column CO_2, Atmos. Chem. Phys., 13(17), 8695–8717, doi:10.5194/acp-13-8695-2013, 2013.

Bisht, J. S. H., Machida, T., Chandra, N., Tsuboi, K., Patra, P. K., Umezawa, T., Niwa, Y., Sawa, Y., Morimoto, S., Nakazawa, T., Saitoh, N. and Takigawa, M.: Seasonal Variations of SF_6, CO_2, CH_4, and N_2O in the UT/LS Region due to Emissions, Transport, and Chemistry, J. Geophys. Res. Atmos., 126(4), 1–18, doi:10.1029/2020JD033541, 2021.

Canadell, J. G., Ciais, P., Gurney, K., Le Quéré, C., Piao, S., Raupach, M. R. and Sabine, C. L.: An International Effort to Quantify Regional Carbon Fluxes, Eos, Trans. Am. Geophys. Union, 92(10), 81–82, doi:10.1029/2011EO100001, 2011.

Chatterjee, A., Gierach, M. M., Sutton, A. J., Feely, R. A., Crisp, D., Eldering, A., Gunson, M. R., O'Dell, C. W., Stephens, B. B. and Schimel, D. S.: Influence of El Niño on atmospheric CO_2 over the tropical Pacific Ocean: Findings from NASA's OCO-2 mission, Science (80-.)., 358(6360), eaam5776, doi:10.1126/science.aam5776, 2017.

Chevallier, F., Ciais, P., Conway, T. J., Aalto, T., Anderson, B. E., Bousquet, P., Brunke, E. G., Ciattaglia, L., Esaki, Y., Fröhlich, M., Gomez, A., Gomez-Pelaez, A. J., Haszpra, L., Krummel, P. B., Langenfelds, R. L., Leuenberger, M., Machida, T., Maignan, F., Matsueda, H., Morguí, J. A., Mukai, H., Nakazawa, T., Peylin, P., Ramonet, M., Rivier, L., Sawa, Y., Schmidt, M., Steele, L. P., Vay, S. A., Vermeulen, A. T., Wofsy, S. and Worthy, D.: CO_2 surface fluxes at grid point scale estimated from a global 21 year reanalysis of atmospheric measurements, J. Geophys. Res., 115(D21), D21307, doi:10.1029/2010JD013887, 2010.

Chevallier, F., Deutscher, N. M., Conway, T. J., Ciais, P., Ciattaglia, L., Dohe, S., Fröhlich, M., Gomez-Pelaez, A. J., Griffith, D., Hase, F., Haszpra, L., Krummel, P., Kyrö, E., Labuschagne, C., Langenfelds, R., Machida, T., Maignan, F., Matsueda, H., Morino, I., Notholt, J., Ramonet, M., Sawa, Y., Schmidt, M., Sherlock, V., Steele, P., Strong, K., Sussmann, R., Wennberg, P., Wofsy, S., Worthy, D., Wunch, D. and Zimnoch, M.: Global CO_2 fluxes inferred from surface air-sample measurements and from TCCON retrievals of the CO_2 total column, Geophys. Res. Lett., 38(24), doi:10.1029/2011GL049899, 2011.

Connor, B. J., Boesch, H., Toon, G., Sen, B., Miller, C. and Crisp, D.: Orbiting Carbon Observatory: Inverse method and prospective error analysis, J. Geophys. Res. Atmos., 113(5), 1–14, doi:10.1029/2006JD008336, 2008.

Conway, T. J., Tans, P. P., Waterman, L. S., Thoning, K. W., Kitzis, D. R., Masarie, K. A. and Zhang, N.: Evidence for interannual variability of the carbon cycle from the National Oceanic and Atmospheric Administration/Climate Monitoring and Diagnostics Laboratory Global Air Sampling Network, J. Geophys. Res., 99(D11), 22831, doi:10.1029/94JD01951, 1994.

Crisp, D., Fisher, B. M., O'Dell, C., Frankenberg, C., Basilio, R., Bösch, H., Brown, L. R., Castano, R., Connor, B., Deutscher, N. M., Eldering, A., Griffith, D., Gunson, M., Kuze, A., Mandrake, L., McDuffie, J., Messerschmidt, J., Miller, C. E., Morino, I., Natraj, V., Notholt, J., O'Brien, D. M., Oyafuso, F., Polonsky, I., Robinson, J., Salawitch, R., Sherlock, V., Smyth, M., Suto, H., Taylor, T. E., Thompson, D. R., Wennberg, P. O., Wunch, D. and Yung, Y. L.: The ACOS CO_2 retrieval algorithm - Part II: Global XCO_2 data characterization, Atmos. Meas. Tech., 5(4), 687–707, doi:10.5194/amt-5-687-2012, 2012.

Crisp, D., Pollock, H., Rosenberg, R., Chapsky, L., Lee, R., Oyafuso, F., Frankenberg, C., Dell, C., Bruegge, C., Doran, G., Eldering, A., Fisher, B., Fu, D., Gunson, M., Mandrake, L., Osterman, G., Schwandner, F., Sun, K., Taylor, T., Wennberg, P. and Wunch, D.: The on-orbit performance of the Orbiting Carbon Observatory-2 (OCO-2) instrument and its radiometrically calibrated products, Atmos. Meas. Tech., 10(1), 59–81, doi:10.5194/amt-10-59-2017, 2017.

Crowell, S., Baker, D., Schuh, A., Basu, S., Jacobson, A. R., Chevallier, F., Liu, J., Deng, F., Feng, L., McKain, K., Chatterjee, A., Miller, J. B., Stephens, B. B., Eldering, A., Crisp, D., Schimel, D., Nassar, R., O'Dell, C. W., Oda, T., Sweeney, C., Palmer, P. I. and Jones, D. B. A.: The 2015–2016 carbon cycle as seen from OCO-2 and the global in situ network, Atmos. Chem. Phys., 19(15), 9797–9831, doi:10.5194/acp-19-9797-2019, 2019.

Dlugokencky, E. and Tans, P.: Trends in Atmospheric Carbon Dioxide, NOAA/GML; www.esrl.noaa.gov/gmd/ccgg/trends/, last access: 7 January 2021.

Feely, R. A., Boutin, J., Cosca, C. E., Dandonneau, Y., Etcheto, J., Inoue, H. Y., Ishii, M., Quéré, C. Le, Mackey, D. J., McPhaden, M., Metzl, N., Poisson, A. and Wanninkhof, R.: Seasonal and interannual variability of CO_2 in the equatorial Pacific, Deep. Res. Part II Top. Stud. Oceanogr., 49(13–14), 2443–2469, doi:10.1016/S0967-0645(02)00044-9, 2002.

Frankenberg, C., Kulawik, S. S., Wofsy, S. C., Chevallier, F., Daube, B., Kort, E. A., O'Dell, C., Olsen, E. T. and Osterman, G.: Using airborne HIAPER pole-to-pole observations (HIPPO) to evaluate model and remote sensing estimates of atmospheric carbon dioxide, Atmos. Chem. Phys., 16(12), 7867–7878, doi:10.5194/acp-16-7867-2016, 2016.

Friedlingstein, P., Jones, M. W., O'Sullivan, M., Andrew, R. M., Hauck, J., Peters, G. P., Peters, W., Pongratz, J., Sitch, S., Le Quéré, C., Bakker, D. C. E., Canadell, J. G., Ciais, P., Jackson, R. B., Anthoni, P., Barbero, L., Bastos, A., Bastrikov, V., Becker, M., Bopp, L., Buitenhuis, E., Chandra, N., Chevallier, F., Chini, L. P., Currie, K. I., Feely, R. A., Gehlen, M., Gilfillan, D., Gkritzalis, T., Goll, D. S., Gruber, N., Gutekunst, S., Harris, I., Haverd, V., Houghton, R. A., Hurtt, G., Ilyina, T., Jain, A. K., Joetzjer, E., Kaplan, J. O., Kato, E., Klein Goldewijk, K., Korsbakken, J. I., Landschützer, P., Lauvset, S. K., Lefèvre, N., Lenton, A., Lienert, S., Lombardozzi, D., Marland, G., McGuire, P. C., Melton, J. R., Metzl, N., Munro, D. R., Nabel, J. E. M. S., Nakaoka, S.-I., Neill, C., Omar, A. M., Ono, T., Peregon, A., Pierrot, D., Poulter, B., Rehder, G., Resplandy, L., Robertson, E., Rödenbeck, C., Séférian, R., Schwinger, J., Smith, N., Tans, P. P., Tian, H., Tilbrook, B., Tubiello, F. N., van der Werf, G. R., Wiltshire, A. J. and Zaehle, S.: Global Carbon Budget 2019, Earth Syst. Sci. Data, 11(4), 1783–1838, doi:10.5194/essd-11-1783-2019, 2019.

Hakkarainen, J., Ialongo, I., Maksyutov, S. and Crisp, D.: Analysis of Four Years of Global XCO_2 Anomalies as Seen by Orbiting Carbon Observatory-2, Remote Sens., 11(7), 850, doi:10.3390/rs11070850, 2019.

Inai, Y., Aoki, S., Honda, H., Furutani, H., Matsumi, Y., Ouchi, M., Sugawara, S., Hasebe, F., Uematsu, M. and Fujiwara, M.: Balloon-borne tropospheric CO_2 observations over the equatorial eastern and western Pacific, Atmos. Environ., 184(December 2017), 24–36, doi:10.1016/j.atmosenv.2018.04.016, 2018.

Inoue, M., Morino, I., Uchino, O., Miyamoto, Y., Yoshida, Y., Yokota, T., Machida, T., Sawa, Y., Matsueda, H., Sweeney, C., Tans, P. P., Andrews, A. E., Biraud, S. C., Tanaka, T., Kawakami, S. and Patra, P. K.: Validation of XCO_2 derived from SWIR spectra of GOSAT TANSO-FTS with aircraft measurement data, Atmos. Chem. Phys, 13, 9771–9788, doi:10.5194/acp-13-9771-2013, 2013.

Intergovernmental Panel on Climate Change (IPCC): Climate Change 2013 - The Physical Science Basis, edited by Intergovernmental Panel on Climate Change, Cambridge University Press, Cambridge., 2013.

Keeling, C. D.Revelle, R.: Effects of El Nino/Southern Oscillation on the Atmospheric Content of Carbon Dioxide, Meteoritics, 20(2), 437–450, 1985.

Kim, J. S., Kug, J. S., Yoon, J. H. and Jeong, S. J.: Increased atmospheric CO_2 growth rate during El Niño driven by reduced terrestrial productivity in the CMIP5 ESMs, J. Clim., 29(24), 8783–8805, doi:10.1175/JCLI-D-14-00672.1, 2016.

Kobayashi, S., Ota, Y., Harada, Y., Ebita, A., Moriya, M., Onoda, H., Onogi, K., Kamahori, H., Kobayashi, C., Endo, H., Miyaoka, K. and Takahashi, K.: The JRA-55 Reanalysis: General Specifications and Basic Characteristics, J. Meteorol. Soc. Japan. Ser. II, 93(1), 5–48, doi:10.2151/jmsj.2015-001, 2015.

Kulawik, S. S., Crowell, S., Baker, D., Liu, J., Mckain, K., Sweeney, C., Biraud, S. C., Wofsy, S., Dell, C. W. O., Wennberg, P. O., Wunch, D., Roehl, M., Deutscher, N. M., Kiel, M., Griffith, D. W. T., Velazco, V. A., Dubey, M. K., Sepulveda, E., Elena, O., Rodriguez, G., Té, Y., Heikkinen, P., Dlugokencky, E. J., Gunson, M. R., Eldering, A., Fisher, B. and Osterman, G. B.: Characterization of OCO-2 and ACOS-GOSAT biases and errors for CO_2 flux estimates, (October), 2019.

Kuze, A., Suto, H., Nakajima, M. and Hamazaki, T.: Thermal and near infrared sensor for carbon observation Fourier-transform spectrometer on the Greenhouse Gases Observing Satellite for greenhouse gases monitoring, Appl. Opt., 48(35), 6716, doi:10.1364/AO.48.006716, 2009.

Laughner, J., Andrews, A., Roche, S., Kiel, M. and Toon, G.: ginput v1.0.7b: GGG2020 prior profile software, CaltechDATA., 2021.

Laughner, J.L.; Kiel, M.; Toon, G.; Andrews, A.; Roche, S.; Wunch, D.; Wennberg, P.O. (in prep). Revised formulation of the TCCON priors for GGG2020.

Liu, J., Bowman, K. W., Schimel, D. S., Parazoo, N. C., Jiang, Z., Lee, M., Bloom, A. A., Wunch, D., Frankenberg, C., Sun, Y., O'Dell, C. W., Gurney, K. R., Menemenlis, D., Gierach, M., Crisp, D. and Eldering, A.: Contrasting carbon cycle responses of the tropical continents to the 2015–2016 El Niño, Science (80-.)., 358(6360), doi:10.1126/science.aam5690, 2017.

Machida, T., Matsueda, H., Sawa, Y., Nakagawa, Y., Hirotani, K., Kondo, N., Goto, K., Nakazawa, T., Ishikawa, K. and Ogawa, T.: Worldwide measurements of atmospheric CO_2 and other trace gas species using commercial airlines, J. Atmos. Ocean. Technol., 25(10), 1744–1754, doi:10.1175/2008JTECHA1082.1, 2008.

Matsueda, H., Inoue, H. Y. and Ishii, M.: Aircraft observation of carbon dioxide at 8-13 km altitude over the Western Pacific from 1993 to 1999, Tellus, Ser. B Chem. Phys. Meteorol., 54(1), 1–21, doi:10.1034/j.1600-0889.2002.00304.x, 2002.

Matsueda, H., Machida, T., Sawa, Y., Nakagawa, Y., Hirotani, K., Ikeda, H., Kondo, N. and Goto, K.: Evaluation of atmospheric CO_2 measurements from new flask air sampling of JAL airliner observations, Pap. Meteorol. Geophys., 59(March), 1–17, doi:10.2467/mripapers.59.1, 2008.

Matsueda, H., Machida, T., Sawa, Y. and Niwa, Y.: Long-term change of CO_2 latitudinal distribution in the upper troposphere, Geophys. Res. Lett., 42(7), 2508–2514, doi:10.1002/2014GL062768, 2015.

Miller, C. E., Crisp, D., DeCola, P. L., Olsen, S. C., Randerson, J. T., Michalak, A. M., Alkhaled, A., Rayner, P., Jacob, D. J., Suntharalingam, P., Jones, D. B. A., Denning, A. S., Nicholls, M. E., Doney, S. C., Pawson, S., Boesch, H., Connor, B. J., Fung, I. Y., O'Brien, D., Salawitch, R. J., Sander, S. P., Sen, B., Tans, P., Toon, G. C., Wennberg, P. O., Wofsy, S. C., Yung, Y. L. and Law, R. M.: Precision requirements for space-based data, J. Geophys. Res. Atmos., 112(D10), 1–19, doi:10.1029/2006JD007659, 2007.

Miyazaki, K., Patra, P. K., Takigawa, M., Iwasaki, T. and Nakazawa, T.: Global-scale transport of carbon dioxide in the troposphere, J. Geophys. Res. Atmos., 113(15), 1–21, doi:10.1029/2007JD009557, 2008.

Morino, I., Tsutsumi, Y., Uchino, O., Ohyama, H., Thi Ngoc Trieu, T., Frey, M. M., Yoshida, Y., Matsunaga, T., Kamei, A., Saito, M. and Noda, H. M.: Status of GOSAT and GOSAT-2 FTS SWIR L2 Product Validation, in The 16th International Workshop on Greenhouse Gas Measurement from Space, pp. 2–5., 2020.

Nakajima, M., Suto, H., Yotsumoto, K., Shiomi, K. and Hirabayashi, T.: Fourier transform spectrometer on GOSAT and GOSAT-2, in International Conference on Space Optics — ICSO 2014, vol. 10563, edited by B. Cugny, Z. Sodnik, and N. Karafolas, p. 2, SPIE., 2017.

Nakazawa, T., MIYASHITA, K., AOKI, S. and TANAKA, M.: Temporal and spatial variations of upper tropospheric and lower stratospheric carbon dioxide, Tellus B, 43(2), 106–117, doi:10.1034/j.1600-0889.1991.t01-1-00005.x, 1991.

Niwa, Y., Patra, P. K., Sawa, Y., MacHida, T., Matsueda, H., Belikov, D., Maki, T., Ikegami, M., Imasu, R., Maksyutov, S., Oda, T., Satoh, M. and Takigawa, M.: Three-dimensional variations of atmospheric CO_2: Aircraft measurements and multi-transport model simulations, Atmos. Chem. Phys., 11(24), 13359–13375, doi:10.5194/acp-11-13359-2011, 2011.

O'Dell, C. W., Connor, B., Bösch, H., O'Brien, D., Frankenberg, C., Castano, R., Christi, M., Eldering, D., Fisher, B., Gunson, M., McDuffie, J., Miller, C. E., Natraj, V., Oyafuso, F., Polonsky, I., Smyth, M., Taylor, T., Toon, G. C., Wennberg, P. O. and Wunch, D.: The ACOS CO_2 retrieval algorithm-Part 1: Description and validation against synthetic observations, Atmos. Meas. Tech., 5(1), 99–121, doi:10.5194/amt-5-99-2012, 2012.

OCO-2 Science Team/Michael Gunson, Annmarie Eldering, 2016. ACOS GOSAT/TANSO-FTS Level 2 bias-corrected XCO_2 and other select fields from the full-physics retrieval aggregated as daily files V7.3. Greenbelt, MD, USA, Goddard Earth Sciences Data and Information Services Center (GES DISC). https://disc.gsfc.nasa.gov/datacollection/ACOS_L2_Lite_FP_7.3.html. Accessed: [4/16/2020].

OCO-2 Science Team/Michael Gunson, Annmarie Eldering, 2018. OCO-2 Level 2 bias-corrected XCO2 and other select fields from the full-physics retrieval aggregated as daily files, Retrospective processing V9r. Greenbelt, MD, USA, Goddard Earth Sciences Data and Information Services Center (GES DISC). https://doi.org/10.5067/W8QGIYNKS3JC. Accessed: [5/7/2020].

OCO-2 Science Team/Michael Gunson, Annmarie Eldering, 2019. ACOS GOSAT/TANSO-FTS Level 2 bias-corrected XCO_2 and other select fields from the full-physics retrieval aggregated as daily files V9r. Greenbelt, MD, USA, Goddard Earth Sciences Data and Information Services Center (GES DISC). https://doi.org/10.5067/VWSABTO7ZII4. Accessed: [8/7/2020].

Patra, P. K., Maksyutov, S., Sasano, Y., Nakajima, H., Inoue, G. and Nakazawa, T.: An evaluation of CO_2 observations with Solar Occultation FTS for Inclined-Orbit Satellite sensor for surface source inversion, J. Geophys. Res. Atmos., 108(D24), n/a-n/a, doi:10.1029/2003JD003661, 2003.

Patra, P. K., Ishizawa, M., Maksyutov, S., Nakazawa, T. and Inoue, G.: Role of biomass burning and climate anomalies for land-atmosphere carbon fluxes based on inverse modeling of atmospheric CO_2, Global Biogeochem. Cycles, 19(3), 1–10, doi:10.1029/2004GB002258, 2005.

Patra, P. K., Takigawa, M., Watanabe, S., Chandra, N., Ishijima, K. and Yamashita, Y.: Improved chemical tracer simulation by MIROC4.0-based atmospheric chemistry-transport model (MIROC4-ACTM), Sci. Online Lett. Atmos., 14, 91–96, doi:10.2151/SOLA.2018-016, 2018.

Rayner, P. J., Law, R. M. and Dargaville, R.: The relationship between tropical CO_2 fluxes and the El Niño-Southern Oscillation, Geophys. Res. Lett., 26(4), 493–496, doi:10.1029/1999GL900008, 1999.

Reuter, M., Bösch, H., Bovensmann, H., Bril, A., Buchwitz, M., Butz, A., Burrows, J. P., O'Dell, C. W., Guerlet, S., Hasekamp, O., Heymann, J., Kikuchi, N., Oshchepkov, S., Parker, R., Pfeifer, S., Schneising, O., Yokota, T. and Yoshida, Y.: A joint effort to deliver satellite retrieved atmospheric CO_2 concentrations for surface flux inversions: the ensemble median algorithm EMMA, Atmos. Chem. Phys., 13(4), 1771–1780, doi:10.5194/acp-13-1771-2013, 2013.

Sawa, Y., Machida, T. and Matsueda, H.: Aircraft observation of the seasonal variation in the transport of CO_2 in the upper atmosphere, J. Geophys. Res. Atmos., 117(D5), doi:10.1029/2011JD016933, 2012.

Umezawa, T., Matsueda, H., Sawa, Y., Niwa, Y., Machida, T. and Zhou, L.: Seasonal evaluation of tropospheric CO_2 over the Asia-Pacific region observed by the CONTRAIL commercial airliner measurements, Atmos. Chem. Phys., 18(20), 14851–14866, doi:10.5194/acp-18-14851-2018, 2018.

Velazco, V. A., Morino, I., Uchino, O., Hori, A., Kiel, M., Bukosa, B., Deutscher, N. M., Sakai, T., Nagai, T., Bagtasa, G., Izumi, T., Yoshida, Y. and Griffith, D. W. T.: TCCON Philippines: First measurement results, satellite data and model comparisons in Southeast Asia, Remote Sens., 9(12), 1–18, doi:10.3390/rs9121228, 2017.

Wang, W., Ciais, P., Nemani, R. R., Canadell, J. G., Piao, S., Sitch, S., White, M. A., Hashimoto, H., Milesi, C. and Myneni, R. B.: Variations in atmospheric CO_2 growth rates coupled with tropical temperature (Proceedings of the National Academy of Sciences of the United States of America (2013) 110, 32 (13061-13066) DOI:10.1073/pnas.1219683110), Proc. Natl. Acad. Sci. U. S. A., 110(37), 15163, doi:10.1073/pnas.1314920110, 2013.

Wilcox, L. J., Hoskins, B. J. and Shine, K. P.: A global blended tropopause based on ERA data. Part I: Climatology, Q. J. R. Meteorol. Soc., 138(664), 561–575, doi:10.1002/qj.951, 2012.

Wofsy, S. C.: HIAPER Pole-to-Pole Observations (HIPPO): fine-grained, global-scale measurements of climatically important atmospheric gases and aerosols, Philos. Trans. R. Soc. A Math. Phys. Eng. Sci., 369(1943), 2073–2086, doi:10.1098/rsta.2010.0313, 2011.

Wofsy, S. C., Afshar, S., Allen, H. M., Apel, E., Asher, E. C., Barletta, B., Bent, J., Bian, H., Biggs, B. C., Blake, D. R., Blake, N., Bourgois, I., Brock, C. A., Brune, W. H., Budney, J. W., Bui, T. P., Butler, A., Campuzano-Jost, P., Chang, C. S., Chin, M., Commane, R., Correa, G., Crounse, J. D., Cullis, P. D., Daube, B. C., Day, D. A., Dean-Day, J. M., Dibb, J. E., Digangi, J. P., Diskin, G. S., Dollner, M., Elkins, J. W., Erdesz, F., Fiore, A. M., Flynn, C. M., Froyd, K., Gesler, D. W., Hall, S. R., Hanisco, T. F., Hannun, R. A., Hills, A. J., Hintsa, E. J., Hoffmann, A., Hornbrook, R. S., Huey, L. G., Hughes, S., Jimenez, J. L., Johnson, B. J., Katich, J. M., Keeling, R., Kim, M. J., Kupc, A., Lait, L. R., Lamarque, J.-F., Liu, H. B., McKain, K., Mclaughlin, R. J., Meinardi, S., Miller, D. O., Montzka, S. A., Moore, F. L., Morgan, E. J., Murphy, D. M., Murray, L. T., Nault, B. A., Neuman, J. A., Newman, P. A., Nicely, J. M., Pan, X., Paplawsky, W., Peischl, J., Prather, M. J., Price, D. J., Ray, E., Reeves, J. M., Richardson, M., Rollins, A. W., Rosenlof, K. H., Ryerson, T. B., Scheuer, E., Schill, G. P., Schroder, J. C., Schwarz, J. P., St.Clair, J. M., Steenrod, S. D., Stephens, B. B., Strode, S. A., Sweeney, C., Tanner, D., Teng, A. P., Thames, A. B., Thompson, C. R., Ullmann, K., Veres, P. R., Vizenor, N., Wagner, N. L., Watt, A., Weber, R., Weinzierl, B., et al.: ATom: Merged Atmospheric Chemistry, Trace Gases, and Aerosols, , doi:10.3334/ORNLDAAC/1581, 2018.

Wunch, D., Toon, G. C., Blavier, J.-F. L., Washenfelder, R. A., Notholt, J., Connor, B. J., Griffith, D. W. T., Sherlock, V. and Wennberg, P. O.: The Total Carbon Column Observing Network, Philos. Trans. R. Soc. A Math. Phys. Eng. Sci., 369(1943), 2087–2112, doi:10.1098/rsta.2010.0240, 2011.

Yamagishi, H., Tohjima, Y., Mukai, H., Nojiri, Y., Miyazaki, C. and Katsumata, K.: Observation of atmospheric oxygen/nitrogen ratio aboard a cargo ship using gas chromatography/thermal conductivity detector, J. Geophys. Res. Atmos., 117(D4), doi:10.1029/2011JD016939, 2012.

Yoshida, Y., Kikuchi, N., Morino, I., Uchino, O., Oshchepkov, S., Bril, A., Saeki, T., Schutgens, N., Toon, G. C., Wunch, D., Roehl, C. M., Wennberg, P. O., Griffith, D. W. T., Deutscher, N. M., Warneke, T., Notholt, J., Robinson, J., Sherlock, V., Connor, B., Rettinger, M., Sussmann, R., Ahonen, P., Heikkinen, P., Kyrö, E., Mendonca, J., Strong, K., Hase, F., Dohe, S. and Yokota, T.: Improvement of the retrieval algorithm for GOSAT SWIR XCO_2 and XCH_4 and their validation using TCCON data, Atmos. Meas. Tech., 6(6), 1533–1547, doi:10.5194/amt-6-1533-2013, 2013.

Zeng, N., Mariotti, A. and Wetzel, P.: Terrestrial mechanisms of interannual CO_2 variability, Global Biogeochem. Cycles, 19(1), 1–15, doi:10.1029/2004GB002273, 2005.